

Non-Clifford symmetry protected topological higher-order cluster states in multi-qubit measurement-based quantum computation

Motohiko Ezawa¹

¹*Department of Applied Physics, The University of Tokyo, 7-3-1 Hongo, Tokyo 113-8656, Japan*

(Dated: February 25, 2026)

A cluster state is a strongly entangled state, which is a source of measurement-based quantum computation. It is generated by applying controlled-Z (CZ) gates to the state $|++\cdots+\rangle$. It is protected by the $\mathbb{Z}_2^{\text{even}} \times \mathbb{Z}_2^{\text{odd}}$ symmetry. By applying general quantum gates to the state $|++\cdots+\rangle$, we systematically obtain a general short-range entangled cluster state. If we use a non-Clifford gate such as the controlled phase-shift gate, we obtain a non-Clifford cluster state. Furthermore, if we use the controlled-controlled Z (CCZ) gate instead of the CZ gate, we obtain non-Clifford cluster states with five-body entanglement. We generalize it to the $C^N Z$ gate, where $(2N+1)$ -body entangled states are generated. The $\mathbb{Z}_2^{\text{even}} \times \mathbb{Z}_2^{\text{odd}}$ symmetry is non-Clifford for $N \geq 3$. We demonstrate that there emerge 2^{2N} fold degenerate ground states for an open chain, indicating the emergence of N free spins at each edge. They can be used as an N -qubit input and an N -qubit output in measurement-based quantum computation. We also study the non-invertible symmetry, the Kennedy-Tasaki transformation and the string-order parameter in addition to the $\mathbb{Z}_2^{\text{even}} \times \mathbb{Z}_2^{\text{odd}}$ symmetry in these models.

I. INTRODUCTION

Quantum computation is a next generation computation based on quantum mechanics[1–3]. A standard method is a gate-based quantum computation[4–6], where a quantum circuit is constructed by sequentially applying quantum gates. On the other hand, there is a measurement-based quantum computation[7, 8]. We first prepare a cluster state, which is a strongly entangled state. Then, we measure some qubits with a certain basis and apply feed-back control. Unitary transformation is carried out by appropriately choosing the basis of the measurement.

We consider a chain made of $2L$ qubits. A one-dimensional cluster state $|\psi\rangle$ is commonly generated[9] by applying the controlled-Z (CZ) gates to the state $\bigotimes_{j=1}^{2L} |+\rangle = |++\cdots+\rangle$,

$$|\psi\rangle = \prod_{j=1}^{2L-1} \text{CZ}_{j,j+1} \bigotimes_{j=1}^{2L} |+\rangle, \quad (1)$$

where $\text{CZ}_{j,j+1}$ represents the CZ gate, whose control qubit is j and target qubit is $j+1$.

The Hamiltonian which has the state $|\psi\rangle$ as the ground state is the ZXZ model[10, 11],

$$\mathcal{H}_{\text{ZXZ}} = - \sum_{j=2}^{2L-1} Z_{j-1} X_j Z_{j+1}, \quad (2)$$

where X_j (Z_j) represents the Pauli gate σ_x (σ_z) acting on the qubit j . It is a simplest example realizing the symmetry-protected topological (SPT) phase[12, 13] protected by the $\mathbb{Z}_2^{\text{even}} \times \mathbb{Z}_2^{\text{odd}}$ symmetry. The ground state is gapped and unique for a closed chain. It is a short-ranged entangled state[14], which is disentangled by a finite-depth local-unitary quantum circuit. On the other hand, the ground state is four-fold degenerate for an open chain. They are used as 2 qubits, which are robust against decoherence preserving the $\mathbb{Z}_2^{\text{even}} \times \mathbb{Z}_2^{\text{odd}}$ symmetry[15]. They form logical qubits in measurement-based quantum computation[7, 8, 16]. For example, the left

qubit acts as an input of information. The quantum computation is done by measuring bulk qubits. Then, the output is readout from the right qubit. Recently, it is recognized[17, 18] that this model is a good example possessing non-invertible symmetry[21, 22]. The cluster state is generated by using entangled photons[23]. The ZXZ model is simulated in quantum computer by employing the method of quantum imaginary-time evolution[24].

In this paper, by using a general quantum gate, we generalize a short-ranged entangled cluster state (1) as

$$|\psi\rangle = \prod_{j=1}^{2L-N} U_{\{j;N\}} \bigotimes_{j=1}^{2L} |+\rangle, \quad (3)$$

where $U_{\{j;N\}}$ is a finite-depth local-unitary N -qubit gate around the qubit j . Then, we construct a cluster Hamiltonian associated with the cluster state (3), which gives a generalized ZXZ model. If we use a non-Clifford gate such as the controlled phase shift (CP) gate as $U_{\{j;N\}}$, we obtain a non-Clifford cluster model. On the other hand, if we use a long-range entangled quantum gate such as the CZ, CCZ and $C^N Z$ gates, we obtain higher-order cluster models with a $(2N+1)$ -body interaction. The $\mathbb{Z}_2^{\text{even}} \times \mathbb{Z}_2^{\text{odd}}$ symmetry and non-invertible symmetry are obtained by a corresponding unitary transformation. It is remarkable that there are 2^{2N} fold degenerate ground states for an open chain, which indicates that N free spins emerge at each edge. They can be used as input and output qubits in measurement-based quantum computation. It is a generalization of the ordinary cluster state, where only single qubit is used for the input and output.

This paper is composed as follows. In Sec.II, we summarize the ZXZ model. It is a frustration free model, where the ground state of the local Hamiltonian constitutes the ground state of the total Hamiltonian, and hence, it is exactly solvable. The $\mathbb{Z}_2^{\text{even}} \times \mathbb{Z}_2^{\text{odd}}$ symmetry and non-invertible symmetry are explained. Especially, the former symmetry protects the four-fold degenerate ground state for an open chain. In Sec.III, we introduce a class of unitary-mapped ZXZ models generated by $U_{\{j;N\}}$. The symmetries are maintained by applying unitary transformations. In Sec.IV, we study the ZXZ

model, which is generated by applying the Hadamard gates to the ZXZ model. In Sec.V, we study the XXX-ZZZ model, which is generated by deleting the Hadamard gate only for the even sites from the ZXZ model. In Sec.VI and VII, we study the effect of random bit flip and phase flip on the ZXZ model. They are non-Clifford cluster models for general angles of the bit and phase flips. It is shown that the cluster state is robust against the bit and phase flips. In Sec.VIII, we study a cluster model generated by the controlled phase-shift (CP) gate. In Sec.IX, we study a higher-order cluster model generated by the CCZ gate, which has five-body interactions of qubits. It is a non-Clifford higher-order cluster model with five-body interactions. It is shown that it is a special class of the model generated by the ZZZ, Ising and Z gates. In Sec.X, we study a cluster model generated by the $C^N Z$ gates with $1 \leq n \leq N$. It is shown that the model has $(2N + 1)$ -body interaction. There emerge 2^{2N} fold degenerate ground states for an open chain, which indicates that N free spins emerge at each edge. They can be used as an N -qubit input and an N -qubit output in measurement-based quantum computation. In Sec. XI, we further generalize a higher-order cluster model to a model generated by $C^N P$ gates. Sec.XII is devoted to discussions.

II. ZXZ MODEL

We first review the cluster state and the ZXZ model[10, 11]. We consider a chain with the length $2L$ where $L \geq 1$. The cluster state is generated by applying the CZ gates to the state $\bigotimes_{j=1}^{2L} |+\rangle$ as

$$|\psi^{\text{ZXZ}}\rangle = \text{CZ} \bigotimes_{j=1}^{2L} |+\rangle, \quad (4)$$

where

$$\text{CZ} \equiv \prod_{j=1}^{2L-1} \text{CZ}_{j,j+1} \quad (5)$$

for an open chain, while

$$\text{CZ} \equiv \prod_{j=1}^{2L} \text{CZ}_{j,j+1} = \text{CZ}_{2L,1} \prod_{j=1}^{2L-1} \text{CZ}_{j,j+1} \quad (6)$$

for a closed chain by identifying the qubit $2L + 1$ with the qubit 1. Here,

$$\begin{aligned} \text{CZ}_{j,j+1} &\equiv 1 - \frac{1-Z_j}{2} \frac{1-Z_{j+1}}{2} \\ &= \text{diag}(1, 1, 1, -1)_{j,j+1} \end{aligned} \quad (7)$$

is the CZ gate acting on the qubits j and $j + 1$.

The state $\bigotimes_{j=1}^{2L} |+\rangle$ is generated by the Hadamard gate as

$$\bigotimes_{j=1}^{2L} |+\rangle = \bigotimes_{j=1}^{2L} H_j |0\rangle, \quad (8)$$

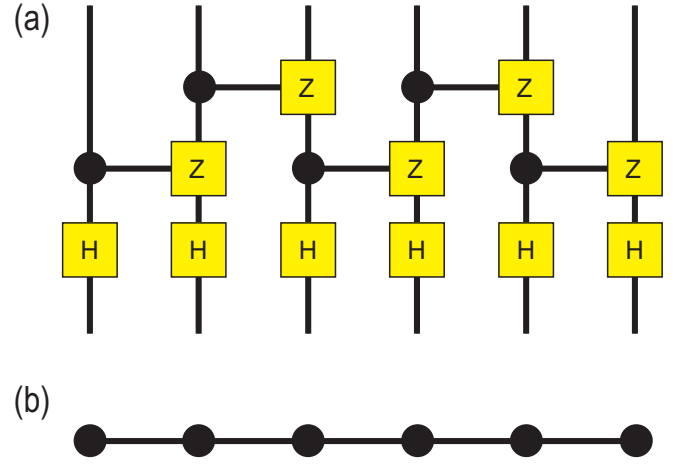


FIG. 1. ZXZ model. (a) Quantum circuit generating the ZXZ cluster state. (b) Its graph representation. The vertices represent the state $|+\rangle$ and the edges represent the CZ gates.

where $|+\rangle = (|0\rangle + |1\rangle) / \sqrt{2}$, and

$$H_j \equiv \frac{1}{\sqrt{2}} \begin{pmatrix} 1 & 1 \\ 1 & -1 \end{pmatrix} \quad (9)$$

is the Hadamard gate acting on the qubit j . The quantum circuit corresponding to Eq.(4) is shown in Fig.1(a). The generated cluster state is called the graph state[8, 25], because all CZ gates commute each other,

$$[\text{CZ}_{j,j+1}, \text{CZ}_{j',j'+1}] = 0, \quad (10)$$

and because the controlled qubit and the target qubit can be replaced in the CZ gate. The graph representation of Eq.(4) is shown in Fig.1(b).

The corresponding cluster Hamiltonian is composed as follows. We start with the Hamiltonian

$$\mathcal{H}_X = - \sum_{j=1}^{2L} X_j, \quad (11)$$

which has the ground state $\bigotimes_{j=1}^{2L} |+\rangle$ because we have $X_j |+\rangle = |+\rangle$, where X_j is the Pauli X operator acting on the qubit j . Then, the Hamiltonian

$$\mathcal{H}_{\text{ZXZ}} \equiv \text{CZ} \mathcal{H}_X \text{CZ} = - \sum_{j=1}^{2L} (\text{CZ}) X_j (\text{CZ}) \quad (12)$$

has the ground state $|\psi^{\text{ZXZ}}\rangle$ given by (4). The Hamiltonians (11) and (12) are used both for an open chain and a closed chain.

An explicit calculation shows that the Hamiltonian is given in the form of

$$\mathcal{H}_{\text{ZXZ}} = - \sum_{j=1}^{2L} K_j^{\text{ZXZ}}, \quad (13)$$

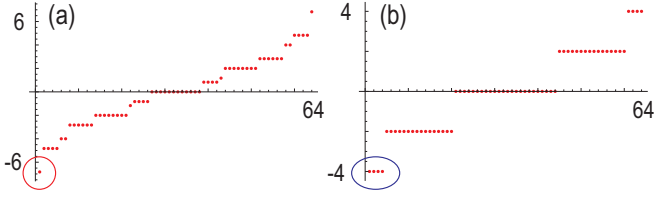


FIG. 2. Energy spectrum of the ZXZ model. (a) Closed chain, where there is a single gapped ground state as indicated by a closed red circle. (b) Open chain, where there are four-fold degenerate gapped ground state as indicated by a closed blue oval. We have set $L = 3$. The vertical axis is the energy, while the horizontal axis is the index of the energy.

where K_j^{ZXZ} are the stabilizers. The explicit forms of the stabilizers depend on an open chain or a closed chain.

The stabilizers satisfy

$$[K_j^{\text{ZXZ}}, K_{j'}^{\text{ZXZ}}] = 0, \quad (K_j^{\text{ZXZ}})^2 = 1. \quad (14)$$

The Hamiltonian (17) is frustration free[27–29], where the ground state $|g\rangle$ satisfies

$$K_j^{\text{ZXZ}} |g\rangle = |g\rangle \quad (15)$$

for all j and the stabilizer state $|g\rangle$. In addition, it is possible to obtain all eigenstates because we have

$$K_j^{\text{ZXZ}} |\psi\rangle = \pm |\psi\rangle. \quad (16)$$

A. Closed chain

For a closed chain, we consider the Hamiltonian \mathcal{H}_{ZXZ} given by

$$\mathcal{H}_{\text{ZXZ}} = - \sum_{j=1}^{2L} K_j^{\text{ZXZ}} \quad (17)$$

by identifying the qubit $j = 2L + 1$ and the qubit $j = 1$, where the stabilizers are given by

$$K_j^{\text{ZXZ}} = Z_{j-1} X_j Z_{j+1} \quad (18)$$

for $2 \leq j \leq 2L - 1$ and

$$K_1^{\text{ZXZ}} = Z_{2L} X_1 Z_2, \quad (19)$$

$$K_{2L}^{\text{ZXZ}} = Z_{2L-1} X_{2L} Z_1. \quad (20)$$

The eigenspectrum for a closed chain is shown in Fig.2(a), where there is a single gapped ground state as indicated by a closed red circle.

B. $\mathbb{Z}_2^{\text{even}} \times \mathbb{Z}_2^{\text{odd}}$ symmetry

The ZXZ Hamiltonian \mathcal{H}_{ZXZ} satisfies

$$[\mathcal{H}_{\text{ZXZ}}, \eta_{\text{ZXZ}}^{\text{even}}] = [\mathcal{H}_{\text{ZXZ}}, \eta_{\text{ZXZ}}^{\text{odd}}] = 0, \quad (21)$$

with

$$\eta_{\text{ZXZ}}^{\text{even}} \equiv \prod_{j \in \text{even}} X_j, \quad \eta_{\text{ZXZ}}^{\text{odd}} \equiv \prod_{j \in \text{odd}} X_j. \quad (22)$$

Because of the relations

$$(\eta_{\text{ZXZ}}^{\text{even}})^2 = (\eta_{\text{ZXZ}}^{\text{odd}})^2 = 1, \quad (23)$$

the Hamiltonian \mathcal{H}_{ZXZ} given by Eq.(17) has the $\mathbb{Z}_2^{\text{even}} \times \mathbb{Z}_2^{\text{odd}}$ symmetry. Consequently, it defines a one-dimensional SPT phase classified by the second cohomology group[19, 20] according to

$$H^2(\mathbb{Z}_2^{\text{even}} \times \mathbb{Z}_2^{\text{odd}}, U(1)) = \mathbb{Z}_2, \quad (24)$$

where $U(1)$ is the group associated with the projective representation of the edge states. See Appendix A for the second cohomology group.

C. Non-invertible symmetry

In addition to the $\mathbb{Z}_2^{\text{even}} \times \mathbb{Z}_2^{\text{odd}}$ symmetry, the Hamiltonian (17) also satisfies the non-invertible symmetry[18, 21, 22],

$$D_{\text{ZXZ}} \mathcal{H}_{\text{ZXZ}} = \mathcal{H}_{\text{ZXZ}} D_{\text{ZXZ}}, \quad (25)$$

whose generator is given by

$$D_{\text{ZXZ}} = T D_{\text{ZXZ}}^{\text{even}} D_{\text{ZXZ}}^{\text{odd}}. \quad (26)$$

Here, the translation symmetry operator T satisfies

$$T X_j T^{-1} = X_{j+1}, \quad T Z_j T^{-1} = Z_{j+1}, \quad (27)$$

and the non-invertible symmetry operators are given by

$$D_{\text{ZXZ}}^{\text{even}} = e^{\frac{\pi i N}{8}} P_{\text{ZXZ}} e^{-\frac{i\pi}{4} X_{2L}} D_{2L-2}^{\text{ZXZ}} \cdots D_4^{\text{ZXZ}} D_2^{\text{ZXZ}}, \quad (28)$$

$$D_{\text{ZXZ}}^{\text{odd}} = e^{\frac{\pi i N}{8}} P_{\text{ZXZ}} e^{-\frac{i\pi}{4} X_{2L-1}} D_{2L-3}^{\text{ZXZ}} \cdots D_3^{\text{ZXZ}} D_1^{\text{ZXZ}} \quad (29)$$

with

$$D_j^{\text{ZXZ}} \equiv e^{-\frac{i\pi}{4} Z_j Z_{j+1}} e^{-\frac{i\pi}{4} X_j}, \quad (30)$$

and the projection operator is given by

$$P_{\text{ZXZ}} \equiv \frac{1 + \eta_{\text{ZXZ}}}{2} \quad (31)$$

with

$$\eta_{\text{ZXZ}} \equiv \eta_{\text{ZXZ}}^{\text{even}} \eta_{\text{ZXZ}}^{\text{odd}}. \quad (32)$$

It is noted that $D_{\text{ZXZ}}^{\text{even}}$ and $D_{\text{ZXZ}}^{\text{odd}}$ do not have inverses due to the projection operator $P \equiv (1 + \eta_{\text{ZXZ}}) / 2$ satisfying $P^2 = P$, which restricts the eigenstates to preserve the $\mathbb{Z}_2^{\text{even}} \times \mathbb{Z}_2^{\text{odd}}$ symmetry. Hence, D_{ZXZ} is called non-invertible symmetry. The non-invertible symmetry D_{ZXZ} maps X_j and $Z_{j-1} Z_{j+1}$ as

$$D_{\text{ZXZ}} X_j = Z_{j-1} Z_{j+1} D_{\text{ZXZ}} \quad (33)$$

$$D_{\text{ZXZ}} Z_{j-1} Z_{j+1} = X_j D_{\text{ZXZ}}, \quad (34)$$

which are abbreviated as

$$X_j \rightsquigarrow Z_{j-1} Z_{j+1}, \quad Z_{j-1} Z_{j+1} \rightsquigarrow X_j, \quad (35)$$

implying that the ZXZ model is self dual under the non-invertible symmetry.

D. Kennedy-Tasaki transformation

The Kennedy-Tasaki (KT) transformation[30–32] maps the SPT model to the Ising model with the next-nearest neighbor interaction,

$$H_{\text{Ising}} \equiv \sum_j Z_{j-1} Z_{j+1}, \quad (36)$$

showing the emergence of a spontaneous symmetry broken phase. The KT transformation for the ZXZ model is defined by[17, 18, 33]

$$\text{KT} \equiv (D_{\text{ZXZ}}^{\text{even}} D_{\text{ZXZ}}^{\text{odd}})^\dagger (\text{CZ}) (D_{\text{ZXZ}}^{\text{even}} D_{\text{ZXZ}}^{\text{odd}})^\dagger, \quad (37)$$

which transforms

$$(\text{KT}) X_j = X_j (\text{KT}), \quad (38)$$

$$(\text{KT}) Z_{j-1} X_j Z_{j+1} = Z_{j-1} Z_{j+1} (\text{KT}). \quad (39)$$

They are abbreviated as

$$X_j \rightsquigarrow X_j, \quad (40)$$

$$Z_{j-1} X_j Z_{j+1} \rightsquigarrow Z_{j-1} Z_{j+1}. \quad (41)$$

Hence, the ZXZ model (17) is transformed to the Ising model (36),

$$H_{\text{ZXZ}} \rightsquigarrow H_{\text{Ising}}, \quad (42)$$

by the KT transformation.

The Ising model do not have a topological phase although the ZXZ model has. This is because topological property is not conserved by the KT transformation because the KT transformation is a nonlocal transformation.

E. String-order parameter

It is possible to define a string-order parameter[31] in the ZXZ model (17) by

$$\begin{aligned} \mathcal{O}(i, j) &\equiv \langle g | \prod_{k=i}^j K_k^{\text{ZXZ}} | g \rangle \\ &= (-1)^{i-j-1} \langle g | Z_i Y_{i+1} \left(\prod_{k=i+2}^{j-2} X_k \right) Y_{j-1} Z_j | g \rangle, \end{aligned} \quad (43)$$

where $|g\rangle$ is the ground state of a given Hamiltonian and we have used Eq.(18). It is 1 for the SPT state $|g\rangle = |\psi^{\text{ZXZ}}\rangle$, which is the ground state of \mathcal{H}_{ZXZ} due to the stabilizer condition Eq.(15), while it is zero for the trivial state $|g\rangle = \bigotimes_{j=1}^{2L} |+\rangle$, which is the ground state of \mathcal{H}_X . In general, the string-order parameter is not quantized.

F. Open chain and edge states

We next consider an open chain whose edge sites are $j = 1$ and $j = 2L$. The stabilizers at the edges are given by

$$K_1^{\text{ZXZ}} = U_{\text{CZ}} X_1 U_{\text{CZ}}^\dagger = X_1 Z_2, \quad (44)$$

$$K_{2L}^{\text{ZXZ}} = U_{\text{CZ}} X_{2L} U_{\text{CZ}}^\dagger = Z_{2L-1} X_{2L}, \quad (45)$$

while those at the bulk are given by[26]

$$K_j^{\text{ZXZ}} = Z_{j-1} X_j Z_{j+1} \quad (46)$$

for $2 \leq j \leq 2L - 1$. The energy spectrum is identical to that of the Hamiltonian (11), because the Hamiltonian is unitary equivalent to the trivial Hamiltonian (11).

In order to see that the ZXZ model has a symmetry protected topological phase, we project the Hamiltonian (13) onto the $\mathbb{Z}_2^{\text{even}} \times \mathbb{Z}_2^{\text{odd}}$ symmetric space,

$$\tilde{\mathcal{H}}_{\text{ZXZ}} = P_{\text{ZXZ}} \mathcal{H}_{\text{ZXZ}} P_{\text{ZXZ}} = - \sum_{j=2}^{2L-1} K_j^{\text{ZXZ}}, \quad (47)$$

where we have used the relation

$$P_{\text{ZXZ}} K_1^{\text{ZXZ}} P_{\text{ZXZ}} = P_{\text{ZXZ}} K_{2L}^{\text{ZXZ}} P_{\text{ZXZ}} = 0. \quad (48)$$

The stabilizers at the edges K_1^{ZXZ} and K_{2L}^{ZXZ} are absent in $\tilde{\mathcal{H}}_{\text{ZXZ}}$. The eigenspectrum for an open chain is shown in Fig.2(b), where there are four-fold degenerate gapped ground state as indicated by a closed blue oval.

It is understood as follows. We make a unitary transformation by the CZ gate,

$$\text{CZ} \tilde{\mathcal{H}}_{\text{ZXZ}} \text{CZ} = - \sum_{j=2}^{2L-1} X_j. \quad (49)$$

There is no operator for the qubits with $j = 1$ and $2L$ in the Hamiltonian. Then, the ground state is

$$|\psi\rangle = |s_1\rangle \otimes \left(\bigotimes_{j=2}^{2L-1} |+\rangle \right) \otimes |s_{2L}\rangle, \quad (50)$$

where we have used

$$X_j |+\rangle = |+\rangle \quad (51)$$

for $2 \leq j \leq 2L - 1$.

Logical qubits are determined as follows. i) The operators commute with all the stabilizers K_j^{ZXZ} , which means that they are centralizers of the group spanned by the stabilizers. ii) They are linearly independent of the stabilizers. iii) They satisfy the Pauli group.

They are explicitly given by

$$X_{\text{left}} \equiv \text{CZ}_{1,2} X_1 \text{CZ}_{1,2} = X_1 Z_2, \quad (52)$$

$$Y_{\text{left}} \equiv \text{CZ}_{1,2} Y_1 \text{CZ}_{1,2} = Y_1 Z_2, \quad (53)$$

$$Z_{\text{left}} \equiv \text{CZ}_{1,2} Z_1 \text{CZ}_{1,2} = Z_1 \quad (54)$$

for the left edge and

$$X_{\text{right}} \equiv CZ_{2L-1,2L} X_{2L} CZ_{2L-1,2L} = X_{2L} Z_{2L-1}, \quad (55)$$

$$Y_{\text{right}} \equiv CZ_{2L-1,2L} Y_{2L} CZ_{2L-1,2L} = Y_{2L} Z_{2L-1}, \quad (56)$$

$$Z_{\text{right}} \equiv CZ_{2L-1,2L} Z_{2L} CZ_{2L-1,2L} = Z_{2L} \quad (57)$$

for the right edge, where we have used the relations

$$CZ_{j,j+1} X_j CZ_{j,j+1} = X_j Z_{j+1}, \quad (58)$$

$$CZ_{j,j+1} X_{j+1} CZ_{j,j+1} = Z_j X_{j+1}. \quad (59)$$

They satisfy the SU(2) commutation relation of the spin.

The $\mathbb{Z}_2^{\text{even}} \times \mathbb{Z}_2^{\text{odd}}$ symmetry is broken at the edge $j = 1$ and $2L$,

$$[X_{\text{left}}, \eta] \neq 0, \quad [X_{\text{right}}, \eta] \neq 0. \quad (60)$$

It is known as the t'Hooft anomaly[34].

G. Topological phase transition

We consider a Hamiltonian interpolating \mathcal{H}_{ZXZ} and \mathcal{H}_X which is given by

$$H(\alpha) = \alpha \mathcal{H}_{\text{ZXZ}} + (1 - \alpha) \mathcal{H}_X \quad (61)$$

with $0 \leq \alpha \leq 1$.

It has a duality generated by the CZ gate,

$$CZ \mathcal{H}(\alpha) CZ = \mathcal{H}(1 - \alpha), \quad (62)$$

where it is self dual at $\alpha = 1/2$. There emerges an enhanced symmetry $\mathbb{Z}_2^{\text{even}} \times \mathbb{Z}_2^{\text{odd}} \times \mathbb{Z}_2^{\text{CZ}}$ symmetry at $\alpha = 1/2$. The energy spectrum for a closed chain is shown as a function of α in Fig.3(a1). The energy spectrum is symmetric at $\alpha = 1/2$, showing the duality relation. The gap between the ground state and the first-excited state closes at $\alpha = 1/2$, indicating a topological phase transition. On the other hand, the energy spectrum becomes asymmetric for an open chain as shown in Fig.3(b1) because \mathbb{Z}_2^{CZ} symmetry is broken at the edges and the ground state degeneracies are different between \mathcal{H}_{ZXZ} and \mathcal{H}_X . The four-fold degenerate edge states do not split for $\alpha < 1/2$ because there is only one spin at one edge. The degeneracy is broken at α slightly smaller than $1/2$, whose reason is a finite-size effect. The degeneracy is broken at $\alpha = 1/2$ for a sufficiently long chain. The string order parameter is shown in Fig.3(c1) as a function of α . It monotonically decreases as the increase of α and jumps at $\alpha = 1/2$, reflecting a topological phase transition.

Topological phase transition occurs at $\alpha = 1/2$. The mechanism is the same as in the Kramers-Wannier duality in the Ising model. There are only two topological distinct phases because of the second group cohomology is \mathbb{Z}_2 . Then, a topological phase transition occurs only once. On the other hand, $H(\alpha)$ and $H(1 - \alpha)$ are connected by the duality transformation as in Eq.(62). Hence, the topological phase transition occurs at $\alpha = 1/2$.

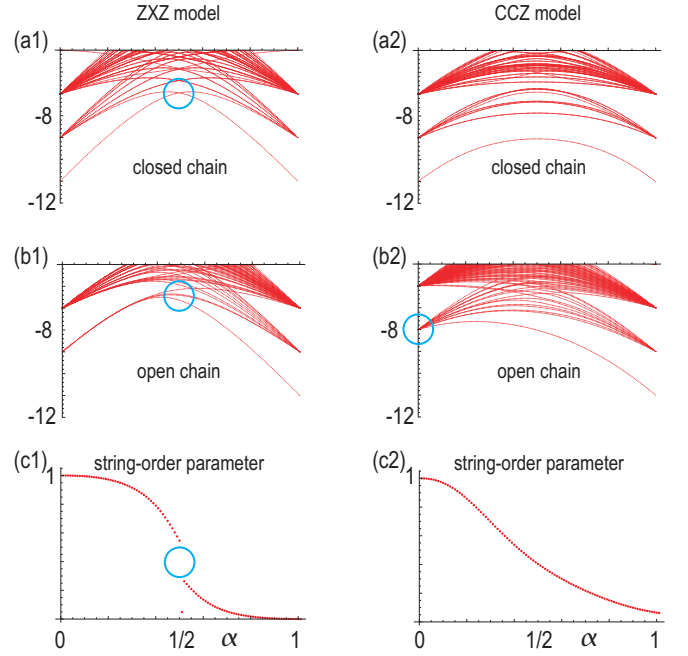


FIG. 3. (a1) Energy spectrum of the ZXZ model for a closed chain. The energy is symmetric at $\alpha = 1/2$ reflecting the \mathbb{Z}_2^{CZ} symmetry. (b1) That for an open chain. The ground states are four-fold degenerate at $\alpha = 0$ and not degenerate at $\alpha = 1$. The degeneracy splits at α slightly smaller than $1/2$. (c1) String order parameter. There is a jump at $\alpha = 1/2$, implying a topological phase transition at $\alpha = 1/2$. (a2) Energy spectrum of the CCZ model for a closed chain. (b2) That for an open chain. The ground states are 16-fold degenerate at $\alpha = 0$ and not degenerate at $\alpha = 1$. The degeneracy splits for $\alpha > 0$. (c2) String order parameter for the CCZ model. There is no jump at $\alpha = 1/2$, implying a topological phase transition at $\alpha = 0$. The horizontal axis is α . We have set $L = 11$

III. UNITARY-MAPPED CLUSTER MODEL

We proceed to generalize the ZXZ model by considering a cluster state generated by

$$|\psi\rangle = \prod_{j=1}^{2L-N} U_{\{j;N\}} \bigotimes_{j=1}^{2L} |+\rangle, \quad (63)$$

where $U_{\{j;N\}}$ is a finite-depth local-unitary N -qubit gate around the qubit j instead of the CZ gate, and $\{j;N\} \equiv \{j, j+1, \dots, j+N\}$ represents the N sequential numbers starting from j . Explicit examples are given later. The corresponding cluster Hamiltonian is constructed as

$$\mathcal{H}_U = - \sum_j K_j \quad (64)$$

with

$$K_j \equiv U_{\{j;N\}} X_j U_{\{j;N\}}^{-1}. \quad (65)$$

It is related to the ZXZ Hamiltonian as

$$\mathcal{H}_U = -V \mathcal{H}_{\text{ZXZ}} V^{-1}, \quad (66)$$

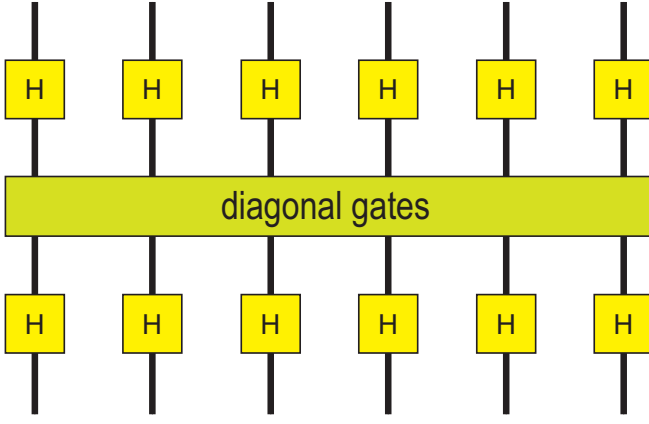


FIG. 4. Quantum circuit for the class of the instantaneous quantum polynomial time (IQP).

where

$$V \equiv \prod_{j=1}^{2L-N} V_{\{j;N\}} \quad (67)$$

with

$$V_{\{j;N\}} \equiv U_{\{j;N\}} CZ_{j,j+1}^{-1}. \quad (68)$$

We obtain a nontrivial Hamiltonian by choosing $U_{\{j;N\}}$. If we choose a non-Clifford gate such as the controlled phase-shift gate as $U_{\{j;N\}}$, we obtain a non-Clifford cluster model. It has the non-Clifford stabilizer state $|g_U\rangle$ as

$$|g_U\rangle \equiv V |g\rangle \quad (69)$$

for the Hamiltonian H_U , satisfying

$$K_j^U |g_U\rangle = |g_U\rangle \quad (70)$$

with

$$K_j^U \equiv V K_j V^{-1}. \quad (71)$$

We note that the original stabilizer state is defined by the Pauli group as in Eq.(18). In addition, it is possible to construct higher-order cluster models by choosing long-range entangled quantum gates.

The generators (22) of the $\mathbb{Z}_2^{\text{even}} \times \mathbb{Z}_2^{\text{odd}}$ symmetry is modified as

$$\eta^{\text{even}} \equiv V \left(\prod_{j \in \text{even}} X_j \right) V^{-1}, \quad \eta^{\text{odd}} \equiv V \left(\prod_{j \in \text{odd}} X_j \right) V^{-1}. \quad (72)$$

The generator (26) of the non-invertible symmetry is modified as

$$D_U = V D_{\text{ZXZ}} V^{-1}. \quad (73)$$

By using the relations

$$V D_{\text{ZXZ}} V^{-1} V X_j V^{-1} = V Z_{j-1} Z_{j+1} V^{-1} V D_{\text{ZXZ}} V^{-1}, \quad (74)$$

$$V D_{\text{ZXZ}} Z_{j-1} V^{-1} V Z_{j+1} V^{-1} = V X_j V^{-1} V D_{\text{ZXZ}} V^{-1}, \quad (75)$$

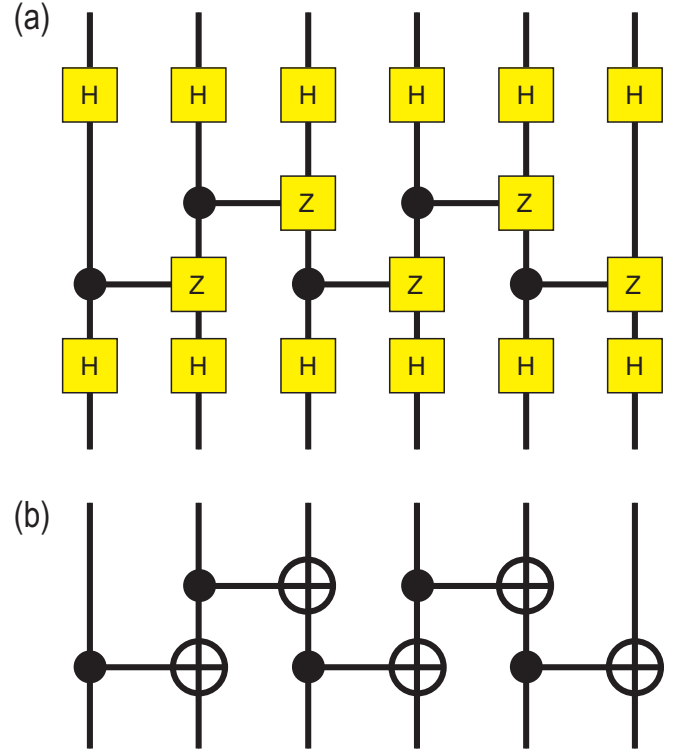


FIG. 5. XZX model. (a) Quantum circuit representation. (b) Equivalent quantum circuit using the CX gates.

we obtain the action of the non-invertible symmetry

$$V X_j V^{-1} \rightsquigarrow V Z_{j-1} Z_{j+1} V^{-1}, \quad (76)$$

$$V Z_{j-1} Z_{j+1} V^{-1} \rightsquigarrow V X_j V^{-1}. \quad (77)$$

Similarly, the action (37) of the KT transformation is modified as

$$V X_j V^{-1} \rightsquigarrow V X_j V^{-1}, \quad (78)$$

$$V Z_{j-1} X_j Z_{j+1} V^{-1} \rightsquigarrow V Z_{j-1} Z_{j+1} V^{-1}. \quad (79)$$

The string-order parameter is modified as

$$\mathcal{O}^U(i, j) \equiv \langle g_U | \prod_{k=i}^j K_k^U | g_U \rangle. \quad (80)$$

We mainly take unitary transformations made by a quantum circuit composed only of diagonal gates and Hadamard gates as shown in Fig.4. This class of quantum circuits is known as the instantaneous quantum polynomial time (IQP) class in the context of quantum information theory[35]. It does not present a universal computation but it is impossible to simulate a quantum circuit in a polynomial time by a classical computer.

IV. XZX MODEL

We next study the XZX model given by[36, 37]

$$\mathcal{H}_{XZX} = - \sum_{j=1}^{2L-1} K_j^{XZX} \quad (81)$$

with the stabilizer

$$K_j^{XZX} \equiv X_{j-1} Z_j X_{j+1}. \quad (82)$$

The Hamiltonian is constructed by applying the Hadamard gates H_j to the ZXZ model (17),

$$\mathcal{H}_{XZX} = \left(\prod_{j=1}^L H_j \right) \mathcal{H}_{ZXZ} \left(\prod_{j=1}^L H_j \right). \quad (83)$$

The associated cluster state is given by

$$|\psi^{XZX}\rangle = \prod_{j=1}^L H_j \prod_{j=1}^{2L-1} CZ_{j,j+1} \bigotimes_{j=1}^L |+\rangle, \quad (84)$$

which corresponds to Eq.(63) with

$$\prod_{j=1}^{2L-N} U_{\{j;N\}} = \prod_{j=1}^L H_j \prod_{j=1}^{2L-1} CZ_{j,j+1}. \quad (85)$$

The quantum circuit representation is shown in Fig.5(a). It is also constructed by simply applying the CNOT gate $CX_{j,j+1}$, whose control qubit is j and target qubit is $j+1$,

$$|\psi^{XZX}\rangle = \prod_{j=1}^{2L-1} CX_{j,j+1} \bigotimes_{j=1}^L |0\rangle. \quad (86)$$

The quantum circuit representation is shown in Fig.5(b).

The generators of the $\mathbb{Z}_2^{\text{even}} \times \mathbb{Z}_2^{\text{odd}}$ symmetry are given by

$$\eta_{XZX}^{\text{even}} \equiv \prod_{j \in \text{even}} Z_j, \quad \eta_{XZX}^{\text{odd}} \equiv \prod_{j \in \text{odd}} Z_j. \quad (87)$$

The generators of the non-invertible symmetry is

$$D_{XZX} = T D_{XZX}^{\text{even}} D_{XZX}^{\text{odd}}, \quad (88)$$

where

$$D_{XZX}^{\text{even}} = e^{\frac{\pi i N}{8}} \frac{1 + \eta_{XZX}}{2} e^{-\frac{i\pi}{4} Z_{2L}} D_{2L-2}^{XZX} \dots D_4^{XZX} D_2^{XZX}, \quad (89)$$

$$D_{XZX}^{\text{odd}} = e^{\frac{\pi i N}{8}} \frac{1 + \eta_{XZX}}{2} e^{-\frac{i\pi}{4} Z_{2L-1}} D_{2L-3}^{XZX} \dots D_3^{XZX} D_1^{XZX} \quad (90)$$

with

$$D_j^{XZX} \equiv e^{-\frac{i\pi}{4} X_j X_{j+1}} e^{-\frac{i\pi}{4} Z_j} \quad (91)$$

and

$$\eta_{XZX} \equiv \eta_{XZX}^{\text{even}} \eta_{XZX}^{\text{odd}}. \quad (92)$$

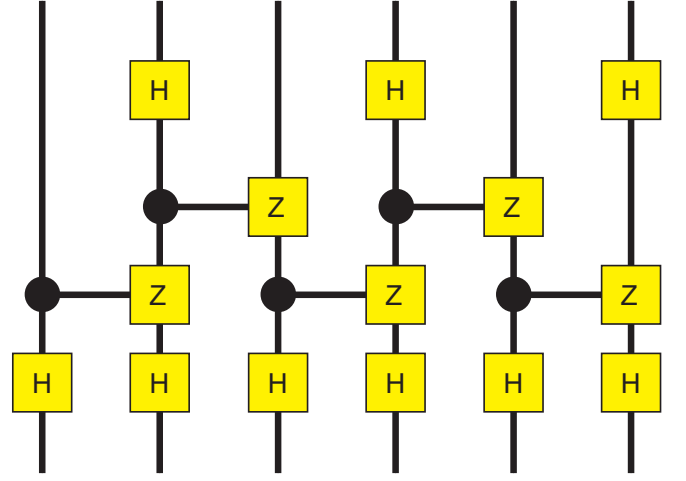


FIG. 6. ZZZ-XXX model. Quantum circuit representation.

The action of the non-invertible symmetry D_{XZX} is

$$Z_j \rightsquigarrow X_{j-1} X_{j+1}, \quad X_{j-1} X_{j+1} \rightsquigarrow Z_j. \quad (93)$$

The action of the KT transformation is

$$Z_j \rightsquigarrow Z_j, \quad (94)$$

$$X_{j-1} Z_j X_{j+1} \rightsquigarrow X_{j-1} X_{j+1}. \quad (95)$$

The string-order parameter is given by

$$\begin{aligned} \mathcal{O}(i, j) &\equiv \langle g | \prod_{k=i}^j K_k^{XZX} | g \rangle \\ &= \langle g | X_i \left(\prod_{k=i+1}^{j-1} Z_k \right) X_j | g \rangle. \end{aligned} \quad (96)$$

V. ZZZ-XXX MODEL

The ZZZ-XXX model is given by[38, 39]

$$\mathcal{H}_{ZZZ} = - \sum_{j=1}^{L-1} (K_{2j}^{ZZZ} + K_{2j+1}^{XXX}) \quad (97)$$

with the stabilizers

$$K_{2j}^{ZZZ} \equiv Z_{2j-1} Z_{2j} Z_{2j+1}, \quad (98)$$

$$K_{2j+1}^{XXX} \equiv X_{2j} X_{2j+1} X_{2j+2}. \quad (99)$$

It is constructed by applying the Hadamard gates only to the even qubits in the ZXZ model,

$$\mathcal{H}_{ZZZ} = \left(\prod_{j=1}^L H_{2j} \right) \mathcal{H}_{ZXZ} \prod_{j=1}^L H_{2j}. \quad (100)$$

The associated cluster state is given by

$$|\psi^{\text{ZZZ}}\rangle = \prod_{j=1}^L H_{2j} \prod_{j=1}^{2L-1} CZ_{j,j+1} \bigotimes_{j=1}^L |+\rangle, \quad (101)$$

which corresponds to Eq.(63) with

$$\prod_{j=1}^{2L-N} U_{\{j;N\}} = \prod_{j=1}^L H_{2j} \prod_{j=1}^{2L-1} CZ_{j,j+1}. \quad (102)$$

$$U_{\{2j;0\}} = H_{2j} \quad (103)$$

$$U_{\{2j-1;0\}} = I_2 \quad (104)$$

$$U_{\{j;1\}} = CZ_{j,j+1} \quad (105)$$

The quantum circuit representation is shown in Fig.6.

The generators of the $\mathbb{Z}_2^{\text{even}} \times \mathbb{Z}_2^{\text{odd}}$ symmetry are given by

$$\eta_{\text{ZZZ}}^{\text{even}} \equiv \prod_{j \in \text{even}} X_j, \quad \eta_{\text{ZZZ}}^{\text{odd}} \equiv \prod_{j \in \text{odd}} Z_j. \quad (106)$$

The generator of the non-invertible symmetry is

$$D_{\text{ZZZ}} = \text{T} D_{\text{ZZZ}}^{\text{even}} D_{\text{ZZZ}}^{\text{odd}}, \quad (107)$$

where

$$D_{\text{ZZZ}}^{\text{even}} = e^{\frac{\pi i N}{8}} \frac{1 + \eta_{\text{ZZZ}}}{2} e^{-\frac{i\pi}{4} Z_{2L}} D_{2L-2}^{\text{ZZZ}} \cdots D_4^{\text{ZZZ}} D_2^{\text{ZZZ}}, \quad (108)$$

$$D_{\text{ZZZ}}^{\text{odd}} = e^{\frac{\pi i N}{8}} \frac{1 + \eta_{\text{ZZZ}}}{2} e^{-\frac{i\pi}{4} X_{2L-1}} D_{2L-2}^{\text{ZZZ}} \cdots D_3^{\text{ZZZ}} D_1^{\text{ZZZ}} \quad (109)$$

with

$$D_{2j}^{\text{ZZZ}} \equiv e^{-\frac{i\pi}{4} X_{2j} Z_{2j+1}} e^{-\frac{i\pi}{4} Z_{2j}}, \quad (110)$$

$$D_{2j-1}^{\text{ZZZ}} \equiv e^{-\frac{i\pi}{4} Z_{2j-1} X_j} e^{-\frac{i\pi}{4} X_{2j-1}} \quad (111)$$

and

$$\eta_{\text{ZZZ}} \equiv \eta_{\text{ZZZ}}^{\text{even}} \eta_{\text{ZZZ}}^{\text{odd}}. \quad (112)$$

The action of the non-invertible symmetry D_{ZZZ} is

$$\begin{aligned} X_{2j-1} &\rightsquigarrow Z_{2j-2} Z_{2j}, & Z_{2j-2} Z_{2j} &\rightsquigarrow X_{2j-1}, \\ Z_{2j} &\rightsquigarrow X_{2j-1} X_{2j+1}, & X_{2j-1} X_{2j+1} &\rightsquigarrow Z_{2j}. \end{aligned} \quad (113)$$

The action of the KT transformation is

$$X_{2j-1} \rightsquigarrow X_{2j-1}, \quad Z_{2j} \rightsquigarrow Z_{2j}, \quad (114)$$

$$Z_{2j-1} Z_{2j} Z_{2j+1} \rightsquigarrow Z_{2j-1} Z_{2j+1}, \quad (115)$$

$$X_{2j} X_{2j+1} X_{2j+2} \rightsquigarrow X_{2j} X_{2j+2}. \quad (116)$$

The string-order parameter is given by

$$\mathcal{O}(i, j) = \langle g | \prod_{k=i}^j K_k | g \rangle. \quad (117)$$

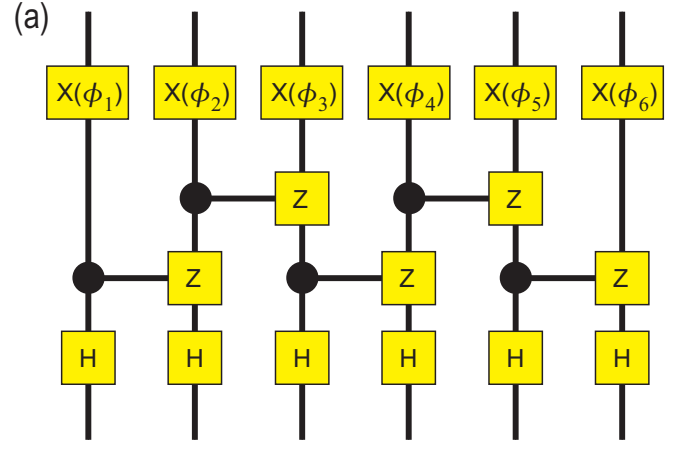


FIG. 7. Bit-flip model. (a) Quantum circuit generating the bit-flipped ZXZ cluster state.

They are explicitly given by

$$\mathcal{O}(i, j) = \langle g | Z_i \left(\prod_{k=i+1}^{j-1} iY_k \right) Z_j | g \rangle \quad (118)$$

for odd i and j ,

$$\mathcal{O}(i, j) = \langle g | X_i \left(\prod_{k=i+1}^{j-1} iY_k \right) X_j | g \rangle \quad (119)$$

for even i and j ,

$$\mathcal{O}(i, j) = \langle g | Z_i \left(\prod_{k=i+1}^{j-1} iY_k \right) X_j | g \rangle \quad (120)$$

for odd i and even j ,

$$\mathcal{O}(i, j) = \langle C | X_i \left(\prod_{k=i+1}^{j-1} iY_k \right) Z_j | C \rangle \quad (121)$$

for even i and odd j .

VI. BIT FLIP MODEL

In actual quantum computer, there is a bit flip error. We model it by the X rotation with an arbitrary angle ϕ_j depending on the site j ,

$$U_{\{j;N\}} = e^{-i\frac{\phi_j}{2} X_j} \equiv U_j^{\text{bit}}, \quad (122)$$

as corresponds to Eq.(63) with $N = 0$. It is a non-Clifford gate. Its action on Z_j is

$$U_j^{\text{bit}} Z_j (U_j^{\text{bit}})^{-1} = Z_j \cos \phi_j - Y_j \sin \phi_j \equiv Z_j(\phi). \quad (123)$$

The generated cluster state is

$$|\psi^{\text{bit}}\rangle = \prod_{j=1}^{2L} U_j^{\text{bit}} \prod_{j=1}^{2L-1} CZ_{j,j+1} \bigotimes_{j=1}^L |+\rangle. \quad (124)$$

The quantum circuit representation is shown in Fig.7. We note that it is not the IQP because U_j^{bit} is not a diagonal gate.

The corresponding Hamiltonian is

$$\mathcal{H}_{\text{bit}} = - \sum_j Z_{j-1}(\phi) X_j Z_{j+1}(\phi). \quad (125)$$

The generators of the $\mathbb{Z}_2^{\text{even}} \times \mathbb{Z}_2^{\text{odd}}$ symmetry are identical to those of the ZXZ model. The generator of the non-invertible symmetry is

$$D_{\text{bit}} = T D_{\text{bit}}^{\text{even}} D_{\text{bit}}^{\text{odd}}, \quad (126)$$

where

$$D_{\text{bit}}^{\text{even}} = e^{\frac{\pi i N}{8}} \frac{1 + \eta_{\text{ZXZ}}}{2} e^{-\frac{i\pi}{4} X_{2L}} D_{2L-2}^{\text{bit}} \cdots D_4^{\text{bit}} D_2^{\text{bit}}, \quad (127)$$

$$D_{\text{bit}}^{\text{odd}} = e^{\frac{\pi i N}{8}} \frac{1 + \eta_{\text{ZXZ}}}{2} e^{-\frac{i\pi}{4} X_{2L-1}} D_{2L-3}^{\text{bit}} \cdots D_3^{\text{bit}} D_1^{\text{bit}} \quad (128)$$

with Eq.(32) and

$$D_j^{\text{bit}} \equiv e^{-\frac{i\pi}{4} Z_j(\phi) Z_{j+1}(\phi)} e^{-\frac{i\pi}{4} X_j}. \quad (129)$$

The action of the non-invertible symmetry D_{bit} is

$$X_j \rightsquigarrow Z_{j-1}(\phi) Z_{j+1}(\phi), \quad (130)$$

$$Z_{j-1}(\phi) Z_{j+1}(\phi) \rightsquigarrow X_j. \quad (131)$$

The four-fold degenerate ground states are robust for an open chain even though we have introduced the site-dependent bit flip.

The action of the KT transformation is

$$X_j \rightsquigarrow X_j, \quad (132)$$

$$Z_{j-1}(\phi) X_j Z_{j+1}(\phi) \rightsquigarrow Z_{j-1}(\phi) Z_{j+1}(\phi). \quad (133)$$

The string-order parameter is given by

$$\begin{aligned} \mathcal{O}(i, j) &\equiv \langle g | \prod_{k=i}^j K_k^{\text{Bit}} | g \rangle \\ &= \langle g | Z_i(\phi) \left(\prod_{k=i+1}^{j-1} X_k \right) Z_j(\phi) | g \rangle. \end{aligned} \quad (134)$$

VII. PHASE FLIP MODEL

In addition to the bit flip, there is also a phase flip in actual quantum computer, which we model by the quantum gate

$$U_j^{\text{phase}} \equiv e^{i\phi_j Z_j}. \quad (135)$$

It is a non-Clifford gate. Its action on X_j is

$$U_j^{\text{phase}} X_j \left(U_j^{\text{phase}} \right)^{-1} = X_j \cos \phi_j - Y_j \sin \phi_j \equiv X_j(\phi_j). \quad (136)$$

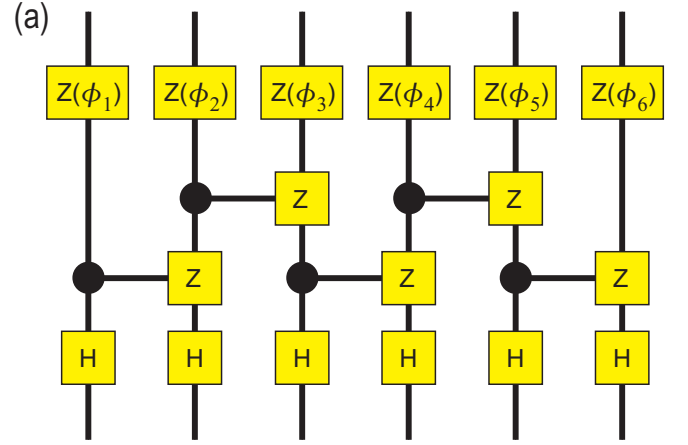


FIG. 8. Phase-flip model. (a) Quantum circuit generating the phase-flipped ZXZ cluster state.

The generated cluster state is

$$|\psi^{\text{phase}}\rangle = \prod_{j=1}^{2L} U_j^{\text{phase}} \prod_{j=1}^{2L-1} CZ_{j,j+1} \bigotimes_{j=1}^L |+\rangle. \quad (137)$$

The quantum circuit representation is shown in Fig.8. The corresponding Hamiltonian is

$$\mathcal{H}_{\text{phase}} = - \sum_j Z_{j-1} X_j(\phi_j) Z_{j+1}. \quad (138)$$

The generators of the $\mathbb{Z}_2^{\text{even}} \times \mathbb{Z}_2^{\text{odd}}$ symmetry are given by

$$\eta_{\text{phase}}^{\text{even}} \equiv \prod_{j \in \text{even}} X_j(\phi_j), \quad \eta_{\text{phase}}^{\text{odd}} \equiv \prod_{j \in \text{odd}} X_j(\phi_j). \quad (139)$$

The generator of the non-invertible symmetry is

$$D_{\text{phase}} = T D_{\text{phase}}^{\text{even}} D_{\text{phase}}^{\text{odd}}, \quad (140)$$

where

$$D_{\text{phase}}^{\text{even}} = e^{\frac{\pi i N}{8}} \frac{1 + \eta_{\text{phase}}}{2} e^{-\frac{i\pi}{4} X_{2L}(\phi)} D_{2L-2}^{\text{phase}} \cdots D_4^{\text{phase}} D_2^{\text{phase}}, \quad (141)$$

$$D_{\text{phase}}^{\text{odd}} = e^{\frac{\pi i N}{8}} \frac{1 + \eta_{\text{bit}}}{2} e^{-\frac{i\pi}{4} X_{2L-1}(\phi)} D_{2L-3}^{\text{phase}} \cdots D_3^{\text{phase}} D_1^{\text{phase}} \quad (142)$$

with

$$D_j^{\text{phase}} \equiv e^{-\frac{i\pi}{4} Z_j Z_{j+1}} e^{-\frac{i\pi}{4} X_j(\phi)} \quad (143)$$

and

$$\eta_{\text{phase}} \equiv \eta_{\text{phase}}^{\text{even}} \eta_{\text{phase}}^{\text{odd}}. \quad (144)$$

The action of the non-invertible symmetry D_{phase} is

$$X_j(\phi) \rightsquigarrow Z_{j-1} Z_{j+1}, \quad Z_{j-1} Z_{j+1} \rightsquigarrow X_j(\phi). \quad (145)$$

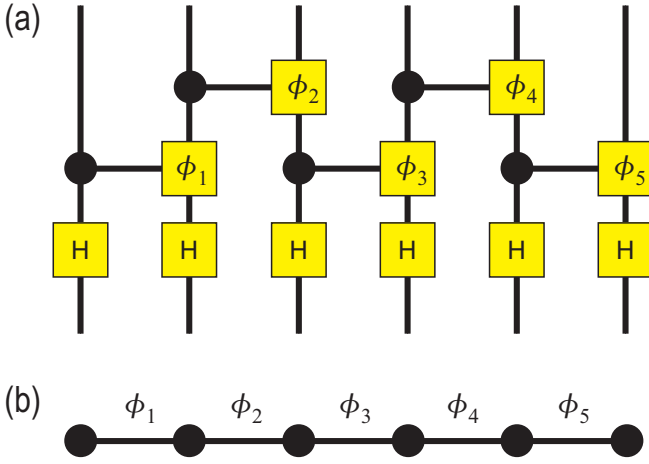


FIG. 9. CP gate model. (a) Quantum circuit representation. (b) Graph representation. The vertices represent the state $|+\rangle$ and the edges represent the CP gates.

The four-fold degenerate ground states are robust for an open chain even though we have introduced the site-dependent phase flip.

The action of the KT transformation is

$$X_j(\phi) \rightsquigarrow X_j(\phi), \quad (146)$$

$$Z_{j-1}X_j(\phi)Z_{j+1} \rightsquigarrow Z_{j-1}Z_{j+1}. \quad (147)$$

The string-order parameter is given by

$$\begin{aligned} \mathcal{O}(i, j) &\equiv \langle g | \prod_{k=i}^j K_k^{\text{phase}} | g \rangle \\ &= \langle g | Z_i \left(\prod_{k=i+1}^{j-1} X_k(\phi) \right) Z_j | g \rangle. \end{aligned} \quad (148)$$

VIII. CONTROLLED PHASE SHIFT GATE MODEL

The CZ gate is actually equipped by time evolution of the CP gate by the fine tuning of $\phi = \pi$. It is hard to precisely tune the phase shift to be $\phi = \pi$ in actual experiments. Hence, it is meaningful to investigate the cluster state generated by the CP gate.

We generalize the cluster state by using the CP gate instead of the CZ gate,

$$\begin{aligned} \text{CP}_{j,j+1}(\phi_j) &\equiv e^{-i\frac{\phi_j}{4}} e^{i\frac{\phi_j}{4} Z_j \otimes I_{j+1}} e^{i\frac{\phi_j}{4} I_j \otimes Z_{j+1}} U_{ZZ}(\phi_j) \\ &= \text{diag}(1, 1, 1, e^{i\phi_j})_{j,j+1}, \end{aligned} \quad (149)$$

where we have assumed a qubit-dependent angle ϕ_j and the Ising gate

$$U_{ZZ}(\phi_j) \equiv e^{-i\frac{\phi_j}{4} Z_j \otimes Z_{j+1}}. \quad (150)$$

See Appendix C for the Ising gate.

It is a non-Clifford gate except for $\phi_j = 0$ and π . The cluster state is generated by

$$|C(\{\phi_j\})\rangle \equiv \prod_{j=1}^{2L-1} \text{CP}_{j,j+1}(\phi_j) \bigotimes_{j=1}^L |+\rangle, \quad (151)$$

which is of the form of Eq.(63) with $N = 1$,

$$\prod_{j=1}^{2L-1} U_{\{j;1\}} = \prod_{j=1}^{2L-1} \text{CP}_{j,j+1}(\phi_j). \quad (152)$$

The quantum circuit representation is shown in Fig.9(a). The generated cluster state is called the weighted graph state[40, 41]. The weighted graph representation is shown in Fig.9(b).

The corresponding Hamiltonian is given by

$$\begin{aligned} \mathcal{H}_{\text{CP}} &= \sum_{j,\{\zeta_j\}} \alpha_{\zeta_{j-1}\zeta_{j+1}} Z_{j-1}^{\zeta_{j-1}} X_j Z_{j+1}^{\zeta_{j+1}} \\ &\quad + \sum_{j,\{v_j\}} \beta_{v_{j-1}v_{j+1}} Y_{j-1}^{v_{j-1}} X_j Y_{j+1}^{v_{j+1}} \end{aligned} \quad (153)$$

with

$$\alpha_{00} = \frac{1}{4} (1 + \cos \phi_j + \cos \phi_{j+1} + \cos(\phi_j + \phi_{j+1})), \quad (154)$$

$$\alpha_{10} = \frac{1}{4} (1 - \cos \phi_j + \cos \phi_{j+1} - \cos(\phi_j + \phi_{j+1})), \quad (155)$$

$$\alpha_{01} = \frac{1}{4} (1 + \cos \phi_j - \cos \phi_{j+1} - \cos(\phi_j + \phi_{j+1})), \quad (156)$$

$$\alpha_{11} = \frac{1}{4} (1 - \cos \phi_j - \cos \phi_{j+1} + \cos(\phi_j + \phi_{j+1})), \quad (157)$$

$$\beta_{00} = \frac{1}{4} (\sin \phi_j + \sin \phi_{j+1} + \sin(\phi_j + \phi_{j+1})), \quad (158)$$

$$\beta_{10} = \frac{1}{4} (-\sin \phi_j + \sin \phi_{j+1} - \sin(\phi_j + \phi_{j+1})), \quad (159)$$

$$\beta_{01} = \frac{1}{4} (\sin \phi_j - \sin \phi_{j+1} - \sin(\phi_j + \phi_{j+1})), \quad (160)$$

$$\beta_{11} = \frac{1}{4} (-\sin \phi_j - \sin \phi_{j+1} + \sin(\phi_j + \phi_{j+1})), \quad (161)$$

where we have used the relation

$$\begin{aligned} &\text{CP}_{j,j+1}(\phi_j) X_{j+1} \text{CP}_{j,j+1}(\phi_j) \\ &= X_{j+1} \cos(\phi_j) + Y_{j+1} \sin(\phi_j). \end{aligned} \quad (162)$$

They are simplified for a constant angle $\phi_j = \phi$ as

$$\alpha_{00} = \cos^2 \frac{\phi}{2} \cos \phi, \quad (163)$$

$$\alpha_{10} = \alpha_{01} = \frac{\sin^2 \phi}{2}, \quad (164)$$

$$\alpha_{11} = -\sin^2 \frac{\phi}{2} \cos \phi, \quad (165)$$

$$\beta_{00} = \cos^2 \frac{\phi}{2} \sin \phi, \quad (166)$$

$$\beta_{10} = \beta_{01} = -\frac{\sin 2\phi}{4}, \quad (167)$$

$$\beta_{11} = -\sin^2 \frac{\phi}{2} \sin \phi. \quad (168)$$

It is interesting that the four-fold degenerate edge states are robust even for small angle rotation ϕ . It is a merit for experimental realization[42], because it is hard to make a large angle rotation $\phi = \pi$.

The action of the non-invertible symmetry is

$$\tilde{X}_j \rightsquigarrow Z_{j-1} Z_{j+1}, \quad Z_{j-1} Z_{j+1} \rightsquigarrow \tilde{X}_j. \quad (169)$$

with

$$\begin{aligned} \tilde{X}_j(\phi) &\equiv X_j \cos \phi \cos^2 \frac{\phi}{2} + Y_j \sin \phi \cos^2 \frac{\phi}{2} \\ &+ (X_j Z_{j+1} + Z_{j-1} X_j) \frac{\sin^2 \phi}{2} \\ &- (Y_j Z_{j+1} + Z_{j-1} Y_j) \frac{\sin 2\phi}{4} \\ &- Z_{j-1} X_j Z_{j+1} \cos \phi \sin^2 \frac{\phi}{2} \\ &- Z_{j-1} Y_j Z_{j+1} \sin \phi \sin^2 \frac{\phi}{2}. \end{aligned} \quad (170)$$

The action of the KT transformation is

$$\tilde{X}_j(\phi) \rightsquigarrow \tilde{X}_j(\phi), \quad (171)$$

$$Z_{j-1} \tilde{X}_j(\phi) Z_{j+1} \rightsquigarrow Z_{j-1} Z_{j+1}. \quad (172)$$

IX. CCZ GATE MODEL

We have so far consider the one-qubit and two-qubit gates. In this section, we consider three-qubit gates. The CCZ gate is defined by

$$\begin{aligned} \text{CCZ}_{j-1,j,j+1} &\equiv 1 - \frac{1 - Z_{j-1}}{2} \frac{1 - Z_j}{2} \frac{1 - Z_{j+1}}{2} \\ &= \text{diag}(1, 1, 1, 1, 1, 1, 1, -1)_{j,j+1} \end{aligned} \quad (173)$$

The CCZ gate is not a Clifford gate. We consider a higher-order cluster state generated by the CCZ gate,

$$|\psi\rangle = \prod_{j=2}^{L-1} \text{CCZ}_{j-1,j,j+1} \bigotimes_{j=1}^L |+\rangle, \quad (174)$$

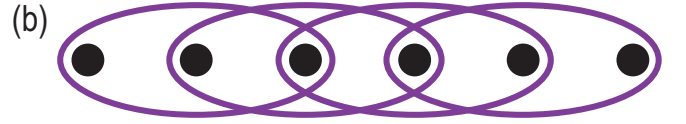
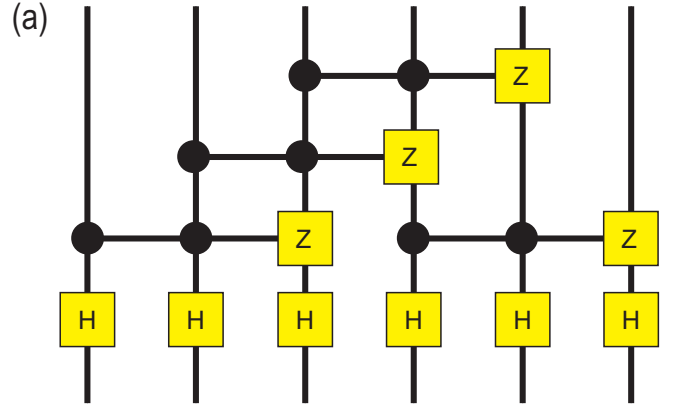


FIG. 10. CCZmodel. (a) Quantum circuit representation. (b) Hyper-graph representation. Ovals including three vertices represent CCZ gates.

which is of the form of Eq.(63) with $N = 2$. The quantum circuit corresponding to Eq.(174) is shown in Fig.10(a). The generated cluster states are called the hyper-graph states[43, 44]. The hyper-graph representation of Eq.(174) is shown in Fig.10(b).

The CCZ gate is decomposed as

$$\begin{aligned} \text{CCZ}_{j-1,j,j+1} &= e^{i\frac{\pi}{8}} e^{-i\frac{\pi}{8} Z_{j-1} \otimes I_j \otimes I_{j+1}} e^{-i\frac{\pi}{8} I_{j-1} \otimes Z_j \otimes I_{j+1}} e^{-i\frac{\pi}{8} I_{j-1} \otimes I_j \otimes Z_{j+1}} \\ &\times e^{i\frac{\pi}{8} Z_{j-1} \otimes Z_j \otimes I_{j+1}} e^{i\frac{\pi}{8} Z_{j-1} \otimes I_j \otimes Z_{j+1}} e^{i\frac{\pi}{8} I_{j-1} \otimes Z_j \otimes Z_{j+1}} \\ &\times e^{-i\frac{\pi}{8} Z_{j-1} \otimes Z_j \otimes Z_{j+1}}. \end{aligned} \quad (175)$$

The product of the CCZ gates is given by

$$\begin{aligned} &\prod_{j=1}^{2L} \text{CCZ}_{j-1,j,j+1} \\ &= e^{i\frac{\pi L}{8}} \prod_{j=1}^{2L} e^{-i\frac{3\pi}{8} Z_j} e^{i\frac{\pi}{4} Z_j \otimes Z_{j+1}} e^{-i\frac{\pi}{8} Z_{j-1} \otimes Z_j \otimes Z_{j+1}}. \end{aligned} \quad (176)$$

Then, the corresponding Hamiltonian has a form

$$H_{\text{CCZ}} = -\sum_j K_j^{\text{CCZ}} \quad (177)$$

with the stabilizer

$$K_j^{\text{CCZ}} = \text{CCZ}_{\{j\}} X_j \text{CCZ}_{\{j\}}, \quad (178)$$

where

$$\text{CCZ}_{\{j\}} \equiv \text{CCZ}_{j-2,j-1,j} \text{CCZ}_{j-1,j,j+1} \text{CCZ}_{j,j+1,j+2}. \quad (179)$$

Especially, the Hamiltonian corresponding to the CCZ gate is given by the stabilizer

$$\begin{aligned}
K_j^{\text{CCZ}} &= \frac{1}{4} \sum_{j=1}^{2L} X_j + \frac{1}{4} \sum_{j=1}^{2L-1} X_j Z_{j+1} + Z_j X_{j+1} \\
&+ \frac{1}{4} \sum_{j=1}^{2L-2} X_j Z_{j+2} + Z_j X_{j+2} \\
&+ \frac{1}{4} \sum_{j=1}^{2L-2} Z_j X_{j+1} Z_{j+2} + X_j Z_{j+1} Z_{j+2} + Z_j Z_{j+1} X_{j+2} \\
&- \frac{1}{4} \sum_{j=1}^{2L-3} Z_j X_{j+1} Z_{j+3} + Z_j X_{j+2} Z_{j+3} \\
&+ \frac{1}{4} \sum_{j=1}^{2L-4} Z_j X_{j+2} Z_{j+4} \\
&- \frac{1}{4} \sum_{j=1}^{2L-3} Z_j Z_{j+1} X_{j+2} Z_{j+3} + Z_j X_{j+1} Z_{j+2} Z_{j+3} \\
&+ \sum_{j=1}^{2L-3} Z_j Z_{j+1} X_{j+2} Z_{j+4} + Z_j X_{j+2} Z_{j+3} Z_{j+4} \\
&- \frac{1}{4} \sum_{j=1}^{2L-4} Z_j Z_{j+1} X_{j+2} Z_{j+3} Z_{j+4}, \tag{180}
\end{aligned}$$

where we have used the relation

$$\text{CCZ}_{abc} X_a \text{CCZ}_{abc} = X_a \text{CZ}_{bc}. \tag{181}$$

It is summarized in the form of

$$K_j^{\text{CCZ}} = \sum_{\{\zeta_j, \nu_j\}} \alpha_{\zeta_j-2, \zeta_j-1, \zeta_j+1, \zeta_j+2} Z_{j-2}^{\zeta_j-2} Z_{j-1}^{\zeta_j-1} X_j Z_{j+1}^{\zeta_j+1} Z_{j+2}^{\zeta_j+2}, \tag{182}$$

where $\zeta_j, \nu_j = 0, 1$ and

$$\begin{aligned}
\alpha_{0000} &= \alpha_{0010} = \alpha_{0100} = \alpha_{0001} = \alpha_{1000} \\
&= \alpha_{0110} = \alpha_{0011} = \alpha_{1100} = \alpha_{1001} \\
&= \alpha_{1101} = \alpha_{1011} = 1/4, \tag{183}
\end{aligned}$$

$$\alpha_{1110} = \alpha_{0111} = \alpha_{1111} = -1/4. \tag{184}$$

We note that it is different from the previous study on a higher-order cluster model with five-body spin interactions[17, 36, 45–49].

The generators of the $\mathbb{Z}_2^{\text{even}} \times \mathbb{Z}_2^{\text{odd}}$ symmetry are given by

$$\eta_{\text{CCZ}}^{\text{even}} = \prod_{j \in \text{even}} \text{CZ}_{j,j+2} \prod_{j \in \text{even}} X_j, \tag{185}$$

$$\eta_{\text{CCZ}}^{\text{odd}} = \prod_{j \in \text{odd}} \text{CZ}_{j,j+2} \prod_{j \in \text{odd}} X_j, \tag{186}$$

where we have used the relation (181).

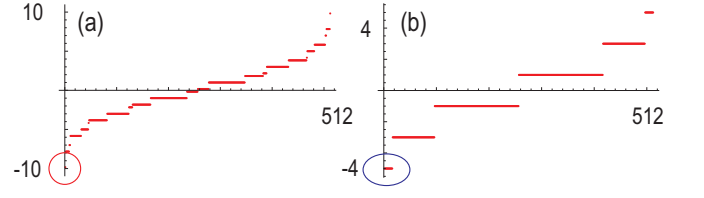


FIG. 11. Energy spectrum of the CCZ model. (a) Closed chain, where there is a single gapped ground state as indicated by a closed red circle. (b) Open chain, where there are 16-fold degenerate gapped ground states as indicated by a closed blue oval. We have set $L = 9$. The vertical axis is the energy, while the horizontal axis is the index of the energy.

A. Edge states

We consider the $\mathbb{Z}_2^{\text{even}} \times \mathbb{Z}_2^{\text{odd}}$ symmetry projected Hamiltonian,

$$\tilde{\mathcal{H}}_{\text{CCZ}} = P H_{\text{CCZ}} P = - \sum_{j=2}^{2L-2} K_j^{\text{CCZ}}. \tag{187}$$

The energy spectrum for an open chain is shown in Fig. 11(b). There is no operator for the qubits with $j = 1, 2, 2L - 1, 2L$ in the Hamiltonian. Then, the ground state is given by

$$|\psi\rangle = |s_1\rangle \otimes |s_2\rangle \otimes \left(\bigotimes_{j=3}^{2L-2} |+\rangle \right) \otimes |s_{2L-1}\rangle \otimes |s_{2L}\rangle. \tag{188}$$

There are 16-fold degenerate states for an open chain because there are only $2L - 2$ stabilizers. It indicates that there are four free spins at edges, where two free spins at one edge. They used as a symmetry-protected topological logical 2-qubit system. They are explicitly given by

$$X_{\text{left}}^1 \equiv \text{CCZ}_{1,2,3} X_1 \text{CCZ}_{1,2,3} = X_1 \text{CZ}_{2,3}, \tag{189}$$

$$Y_{\text{left}}^1 \equiv \text{CCZ}_{1,2,3} Y_1 \text{CCZ}_{1,2,3} = Y_1 \text{CZ}_{2,3}, \tag{190}$$

$$Z_{\text{left}}^1 \equiv \text{CCZ}_{1,2,3} Z_1 \text{CCZ}_{1,2,3} = Z_1, \tag{191}$$

and

$$\begin{aligned}
X_{\text{left}}^2 &\equiv \text{CCZ}_{2,3,4} \text{CCZ}_{1,2,3} X_2 \text{CCZ}_{1,2,3} \text{CCZ}_{2,3,4} \\
&= X_2 \text{CZ}_{2,3} \text{CZ}_{3,4}, \tag{192}
\end{aligned}$$

$$\begin{aligned}
Y_{\text{left}}^2 &\equiv \text{CCZ}_{2,3,4} \text{CCZ}_{1,2,3} Y_2 \text{CCZ}_{1,2,3} \text{CCZ}_{2,3,4} \\
&= Y_2 \text{CZ}_{2,3} \text{CZ}_{3,4}, \tag{193}
\end{aligned}$$

$$\begin{aligned}
Z_{\text{left}}^2 &\equiv \text{CCZ}_{2,3,4} \text{CCZ}_{1,2,3} Z_2 \text{CCZ}_{1,2,3} \text{CCZ}_{2,3,4} \\
&= Z_2 \tag{194}
\end{aligned}$$

for the left edge, while

$$\begin{aligned}
X_{\text{right}}^1 &\equiv \text{CCZ}_{2L-2,2L-1,2L} X_{2L} \text{CCZ}_{2L-2,2L-1,2L} \\
&= X_{2L} \text{CZ}_{2L-1}, \tag{195}
\end{aligned}$$

$$\begin{aligned}
Y_{\text{right}}^1 &\equiv \text{CCZ}_{2L-2,2L-1,2L} Y_{2L} \text{CCZ}_{2L-2,2L-1,2L} \\
&= Y_{2L} \text{CZ}_{2L-1}, \tag{196}
\end{aligned}$$

$$\begin{aligned}
Z_{\text{right}}^1 &\equiv \text{CCZ}_{2L-2,2L-1,2L} Z_{2L} \text{CCZ}_{2L-2,2L-1,2L} \\
&= Z_{2L}, \tag{197}
\end{aligned}$$

and

$$\begin{aligned} X_{\text{right}}^2 &\equiv \text{CCZ}_{2L-2,2L-1,2L} \text{CCZ}_{2L-3,2L-2,2L-1} \\ &\quad \times X_{2L-1} \text{CCZ}_{2L-3,2L-2,2L-1} \text{CCZ}_{2L-2,2L-1,2L} \\ &= X_{2L-1} \text{CZ}_{2L,2L-2} \text{CZ}_{2L-1,2L-2}, \end{aligned} \quad (198)$$

$$\begin{aligned} Y_{\text{right}}^2 &\equiv \text{CCZ}_{2L-2,2L-1,2L} \text{CCZ}_{2L-3,2L-2,2L-1} \\ &\quad \times Y_{2L-1} \text{CCZ}_{2L-3,2L-2,2L-1} \text{CCZ}_{2L-2,2L-1,2L} \\ &= Y_{2L-1} \text{CZ}_{2L,2L-2} \text{CZ}_{2L-1,2L-2}, \end{aligned} \quad (199)$$

$$\begin{aligned} Z_{\text{right}}^2 &\equiv \text{CCZ}_{2L-2,2L-1,2L} \text{CCZ}_{2L-3,2L-2,2L-1} \\ &\quad \times Z_{2L-1} \text{CCZ}_{2L-3,2L-2,2L-1} \text{CCZ}_{2L-2,2L-1,2L} \\ &= Z_{2L-1} \end{aligned} \quad (200)$$

for the right edge.

B. Topological phase transition

As in the case of the ZXZ model, we consider a Hamiltonian interpolating \mathcal{H}_{CCZ} and \mathcal{H}_X ,

$$H(\alpha) = \alpha \mathcal{H}_{\text{CCZ}} + (1 - \alpha) \mathcal{H}_X. \quad (201)$$

It has a duality

$$\text{CCZH}(\alpha) \text{CCZ} = H(1 - \alpha), \quad (202)$$

where it is self dual at $\alpha = 1/2$. There emerges an enhanced symmetry $\mathbb{Z}_2^{\text{even}} \times \mathbb{Z}_2^{\text{odd}} \times \mathbb{Z}_2^{\text{CCZ}}$ symmetry at $\alpha = 1/2$. The energy spectrum for a closed chain is shown as a function of α in Fig.3(a2). The energy spectrum is symmetric at $\alpha = 1/2$, showing the duality relation. As opposed to the ZXZ model, the gap between the ground state and the first-excited state does not close at $\alpha = 1/2$. The energy spectrum becomes asymmetric for an open chain as shown in Fig.3(b2) because $\mathbb{Z}_2^{\text{CCZ}}$ symmetry is broken at the edges, and the ground state degeneracies are different between \mathcal{H}_{ZXZ} and \mathcal{H}_X . The 16-fold degenerate edge states split to 2-fold degenerate edge states for $\alpha > 0$. It is because there are two spins at one edge, which interfere between them by \mathcal{H}_X .

The string order parameter is shown in Fig.3(c2) as a function of α . It monotonically decreases as the increase of α . However, there is no jump at $\alpha = 1/2$. These facts indicate that a topological phase transition occurs at $\alpha = 0$, which is contrasted to the ZXZ model as in Fig.3.

X. C^NZ GATE MODEL

We consider a higher-order cluster state generated by the C^NZ gate[44],

$$|\psi\rangle = \prod_{j=1}^{2L-N} \text{C}^N \text{Z}_{\{j;N\}} \bigotimes_{j=1}^{2L} |+\rangle_j, \quad (203)$$

which is of the form of Eq.(63), where the C^NZ gate is defined by

$$\text{C}^N \text{Z}_{\{j;N\}} \equiv 1 - \bigotimes_{k=0}^N \frac{1 - Z_{j+k}}{2}, \quad (204)$$

and $\{j;N\} \equiv \{j, j+1, \dots, j+N\}$ represents the N sequential numbers starting from j . The generated cluster states are called the hyper-graph states[44].

The corresponding Hamiltonian is given by

$$\mathcal{H}_{\text{C}^N\text{Z}} = - \sum_j K_j^{\text{C}^N\text{Z}} \quad (205)$$

with the stabilizer

$$K_j^{\text{C}^N\text{Z}} = \text{C}^N \text{Z}_{\{j\}} \text{X}_j \text{C}^N \text{Z}_{\{j\}}, \quad (206)$$

where

$$\text{C}^N \text{Z}_{\{j\}} \equiv \prod_{k=0}^N \text{C}^N \text{Z}_{\{j-N+k;N\}}. \quad (207)$$

It is explicitly written in the form of

$$\begin{aligned} &K_j^{\text{C}^N\text{Z}} \\ &= \sum_{\{\zeta_j\}} \alpha_{\zeta_{j-N} \dots \zeta_{j-1} \zeta_{j+1} \dots \zeta_{j+N}} \left(\prod_{n=1}^N Z_{j-n}^{\zeta_{j-n}} \right) \text{X}_j \prod_{n=1}^N Z_{j+n}^{\zeta_{j+n}}, \end{aligned} \quad (208)$$

where $\zeta_j = 0, 1$ and the coefficient is

$$\alpha_{\zeta_{j-N} \dots \zeta_{j-1} \zeta_{j+1} \dots \zeta_{j+N}} = \pm \frac{1}{2^N}. \quad (209)$$

The $\text{C}^N\text{Z}_{j,j+1}$ gate is not a Clifford gate for $N \geq 2$. The coefficients are determined as in the case of the CCZ gate by using the N -body Z^N interactions. The generalization to the C^NP gate is straightforward and the stabilizer has the same form with different coefficients.

The $\mathbb{Z}_2^{\text{even}} \times \mathbb{Z}_2^{\text{odd}}$ symmetry is written in the form of

$$\eta_{\text{C}^N\text{Z}}^{\text{even}} = \prod_{j \in \text{even}} \prod_{k=0}^N \text{C}^{N-1} \text{Z}_{\{j\}_k^N - j} \text{X}_j, \quad (210)$$

where $\{j\}_k^N \equiv \{j - N + k; N\}$, while $\{j\}_k^N - j$ represents the difference set of $\{j\}_k^N$ and j . In this derivation, we have used the relation

$$\begin{aligned} &\left(\prod_{k=0}^N \text{C}^N \text{Z}_{\{j\}_k^N} \right) \text{X}_j \left(\prod_{k=0}^N \text{C}^N \text{Z}_{\{j\}_k^N} \right) \\ &= \text{X}_j \prod_{k=0}^N \text{C}^{N-1} \text{Z}_{\{j\}_k^N - j}. \end{aligned} \quad (211)$$

Hence, it is non-Clifford for $N \geq 3$ because the C^NZ gate is not Clifford for $N \geq 2$.

There is a unique ground state for a closed chain because there are L stabilizers $K_j^{\text{C}^N\text{Z}}$ for $1 \leq j \leq L$, where j is defined in the modulo of L .

A. Edge states

We consider the $\mathbb{Z}_2^{\text{even}} \times \mathbb{Z}_2^{\text{odd}}$ symmetry projected Hamiltonian,

$$\tilde{H}_{C^N Z} = P H_{C^N Z} P = - \sum_{j=N}^{2L-N} K_{\{j\}}^{C^N Z}. \quad (212)$$

We make a unitary transformation

$$\begin{aligned} & C^N Z \mathcal{H}_{Z X Z} C^N Z \\ &= - \sum_{j=N+1}^{2L-N-1} \left(\prod_{k=0}^N C^{N-1} Z_{\{j\}_k^{N-j}} \right) X_j \prod_{k=0}^N C^{N-1} Z_{\{j\}_k^{N-j}}. \end{aligned} \quad (213)$$

The ground state is explicitly given by

$$|\psi\rangle = \left(\bigotimes_{j=1}^N |s_j\rangle \right) \otimes \left(\bigotimes_{j=N+1}^{2L-N-1} |+\rangle \right) \otimes \left(\bigotimes_{j=2L-N}^{2L} |s_j\rangle \right). \quad (214)$$

There are 2^{2N} -fold degenerate states for an open chain because there are only $L - 2N$ stabilizers $K_j^{C^N Z}$ for $N + 1 \leq j \leq L - N$. It shows that there are N free spins at each edge. They are used as a symmetry-protected topological N -qubit system protected by the $\mathbb{Z}_2^{\text{even}} \times \mathbb{Z}_2^{\text{odd}}$ symmetry.

The logical qubits are explicitly obtained as

$$X_{\text{left}}^1 = C^N Z_{1,\dots,N} X_1 C^N Z_{1,\dots,N} = X_1 C^{N-1} Z_{2,\dots,N}, \quad (215)$$

$$Y_{\text{left}}^1 = C^N Z_{1,\dots,N} Y_1 C^N Z_{1,\dots,N} = Y_1 C^{N-1} Z_{2,\dots,N}, \quad (216)$$

$$\begin{aligned} X_{\text{left}}^2 &= C^N Z_{2,\dots,N+1} C^N Z_{1,\dots,N} X_2 C^N Z_{2,\dots,N+1} \\ &= X_2 C^{N-1} Z_{2,\dots,N} C^{N-1} Z_{1,\dots,N-1}, \end{aligned} \quad (217)$$

$$\begin{aligned} Y_{\text{left}}^2 &= C^N Z_{2,\dots,N+1} C^N Z_{1,\dots,N} Y_2 C^N Z_{2,\dots,N+1} \\ &= Y_2 C^{N-1} Z_{2,\dots,N} C^{N-1} Z_{1,\dots,N-1}, \end{aligned} \quad (218)$$

⋮

$$X_{\text{left}}^n = \prod_j C^{N-1} Z_{\{j;N\}-n} X_n = X_n \prod_j C^{N-1} Z_{\{j;N\}-n}, \quad (219)$$

$$Y_{\text{left}}^n = \prod_j C^{N-1} Z_{\{j;N\}-n} Y_n = Y_n \prod_j C^{N-1} Z_{\{j;N\}-n}, \quad (220)$$

and

$$Z_{\text{left}}^j = Z_j. \quad (221)$$

XI. $C^N P$ GATE MODEL

In the similar way, the Hamiltonian corresponding to the $C^N P$ gate is given by

$$\mathcal{H}_{C^N P} = - \sum_j K_j^{C^N P} \quad (222)$$

with the stabilizer

$$K_j^{C^N P} = C^N P_{\{j\}} X_j C^N P_{\{j\}} \quad (223)$$

where

$$C^N P_{\{j\}} \equiv \prod_{k=0}^N C^{N-1} P_{\{j;N\}}, \quad (224)$$

with

$$\begin{aligned} & C^{N-1} P_{j-N+k,\dots,j+k} \\ &= \text{diag} (1, 1, \dots, 1, e^{i\phi_j})_{j-N+k,\dots,j+k}. \end{aligned} \quad (225)$$

The cluster state is given by

$$|\psi\rangle = \prod_{j=1}^{2L-N} C^N P_{\{j;N\}} \bigotimes_{j=1}^{2L} |+\rangle_j, \quad (226)$$

which is of the form of Eq.(63).

XII. DISCUSSIONS

We have shown that symmetry protected N -qubits are generated as edge states in higher-order cluster models. They are used as an N -qubit input and an N -qubit output in measurement-based quantum computation. Non-Clifford cluster states will enhance computational ability of a quantum computer although it is not a universal quantum computer[50, 51]. The reason that it is impossible to achieve universal quantum computation with the use of non-Clifford cluster states is that all of the states are well described by matrix product states in one dimension, and hence the system is well simulated by a classical computer[52].

We discuss experimental realizations. The CP gate is constructed by using the Ising gate as shown in Appendix C. Especially, the cross-resonance gate[53] is used in transmon-type superconducting qubits[54, 55] and the Mølmer-Sørensen gate[56] is used in qubits made of ion trap[57]. It is generated in photonic qubits[58] and photonic systems[59]. The CCZ gate is generated by entangled photons[60], superconducting qubits[61] and Rydberg ions[62]. The CCP gate is generated in superconducting qubits[63]. The $C^N Z$ gate is generated in Rydberg Ions[64, 65].

The author is grateful to R. Kobayashi, H. Watanabe and H. Yagi for helpful discussions on the subject. This work is supported by CREST, JST (Grants No. JPMJCR20T2) and Grants-in-Aid for Scientific Research from MEXT KAKENHI (Grant No. 23H00171).

XIII. APPENDIX

A. Second cohomology group

The generators of the $\mathbb{Z}_2^{\text{even}} \times \mathbb{Z}_2^{\text{odd}}$ symmetry (22) form a group G , which have four components,

$$G = \{e, \eta_{\text{odd}}, \eta_{\text{even}}, \eta_{\text{odd}}\eta_{\text{even}}\}. \quad (227)$$

The one-dimensional SPT phase is classified by the second cohomology group[19, 20],

$$H^2(G, U(1)) = \mathbb{Z}_2 \quad (228)$$

for $G = \mathbb{Z}_2 \times \mathbb{Z}_2$. The 2-cochain is defined by

$$\omega : G \times G \rightarrow U(1), \quad (229)$$

It is a 2-cocycle if the condition

$$\omega(g, h)\omega(gh, k) = \omega(h, k)\omega(g, hk) \quad (230)$$

is satisfied. The projective representation is characterized by $\omega(g, h)$ defined by

$$U(g)U(h) = \omega(g, h)U(gh). \quad (231)$$

In usual representation of the group, the representation is linear representation,

$$U(g)U(h) = U(gh), \quad (232)$$

where $\omega(h, k) = 1$. It corresponds to the trivial representation. On the other hand, $\omega(h, k) = -1$ at the edge, which corresponds to the topological representation. The cocycle condition is automatically satisfied if the associated law is satisfied because

$$\begin{aligned} U(g)U(h)U(k) &= \omega(g, h)U(gh)U(k) \\ &= \omega(g, h)\omega(gh, k)U(ghk) \end{aligned} \quad (233)$$

and

$$\begin{aligned} U(g)U(h)U(k) &= U(g)\omega(h, k)U(hk) \\ &= \omega(g, hk)\omega(h, k)U(ghk) \end{aligned} \quad (234)$$

lead to the cocycle condition

$$\omega(g, h)\omega(gh, k) = \omega(g, hk)\omega(h, k). \quad (235)$$

The explicit representation of ω is determined as follows. The projective representations of the edge states are given by

$$U_{\text{left}}(\eta_{\text{ZXZ}}^{\text{odd}}) = X_{\text{left}}, \quad U_{\text{left}}(\eta_{\text{ZXZ}}^{\text{even}}) = Z_{\text{left}}, \quad (236)$$

$$U_{\text{right}}(\eta_{\text{ZXZ}}^{\text{odd}}) = Z_{\text{right}}, \quad U_{\text{right}}(\eta_{\text{ZXZ}}^{\text{even}}) = X_{\text{right}}, \quad (237)$$

as shown in Appendix B.

The edge states have a projective representation,

$$U_{\text{left}}(\eta_{\text{ZXZ}}^{\text{odd}})U_{\text{left}}(\eta_{\text{ZXZ}}^{\text{even}}) = -U_{\text{left}}(\eta_{\text{ZXZ}}^{\text{even}})U_{\text{left}}(\eta_{\text{ZXZ}}^{\text{odd}}), \quad (238)$$

$$U_{\text{right}}(\eta_{\text{ZXZ}}^{\text{odd}})U_{\text{right}}(\eta_{\text{ZXZ}}^{\text{even}}) = -U_{\text{right}}(\eta_{\text{ZXZ}}^{\text{even}})U_{\text{right}}(\eta_{\text{ZXZ}}^{\text{odd}}), \quad (239)$$

with

$$\omega(\eta_{\text{ZXZ}}^{\text{odd}}, \eta_{\text{ZXZ}}^{\text{even}}) = -1. \quad (240)$$

On the other hand, all other pair give a trivial result

$$\omega = 1. \quad (241)$$

B. Projective representation of the ZXZ model

We summarize explicit projective representations of the edge states. The action of the $\mathbb{Z}_{\text{ZXZ}}^{\text{even}}$ symmetry to the left logical qubits reads

$$\begin{aligned} \eta_{\text{ZXZ}}^{\text{even}} X_{\text{left}} \eta_{\text{ZXZ}}^{\text{even}} &= \left(\prod_{j \in \text{even}} X_j \right) X_1 Z_2 \left(\prod_{j \in \text{even}} X_j \right) \\ &= X_1 X_2 Z_2 X_2 = -X_1 Z_2 = -X_{\text{left}} \end{aligned} \quad (242)$$

and

$$\begin{aligned} \eta_{\text{ZXZ}}^{\text{even}} Z_{\text{left}} \eta_{\text{ZXZ}}^{\text{even}} &= \left(\prod_{j \in \text{even}} X_j \right) Z_1 \left(\prod_{j \in \text{even}} X_j \right) \\ &= Z_1 = Z_{\text{left}}, \end{aligned} \quad (243)$$

Then, the representation of the $\mathbb{Z}_{\text{ZXZ}}^{\text{even}}$ symmetry at the left edge is given by

$$U_{\text{left}}(\eta_{\text{ZXZ}}^{\text{even}}) = Z_{\text{left}}. \quad (244)$$

Similarly, the action of the $\mathbb{Z}_{\text{ZXZ}}^{\text{odd}}$ symmetry to the left logical qubits reads

$$\begin{aligned} \eta_{\text{ZXZ}}^{\text{odd}} X_{\text{left}} \eta_{\text{ZXZ}}^{\text{odd}} &= \left(\prod_{j \in \text{odd}} X_j \right) X_1 Z_2 \left(\prod_{j \in \text{odd}} X_j \right) \\ &= X_1 Z_2 = X_{\text{left}} \end{aligned} \quad (245)$$

and

$$\begin{aligned} \eta_{\text{ZXZ}}^{\text{odd}} Z_{\text{left}} \eta_{\text{ZXZ}}^{\text{odd}} &= \left(\prod_{j \in \text{odd}} X_j \right) Z_1 Z_2 \left(\prod_{j \in \text{odd}} X_j \right) \\ &= X_1 Z_1 X_1 Z_2 = -Z_1 Z_2 = -Z_{\text{left}}. \end{aligned} \quad (246)$$

Then, the representation of the $\mathbb{Z}_{\text{ZXZ}}^{\text{odd}}$ symmetry at the left edge is given by

$$U_{\text{left}}(\eta_{\text{ZXZ}}^{\text{odd}}) = X_{\text{left}}. \quad (247)$$

The action of the $\mathbb{Z}_{ZZ}^{\text{even}}$ symmetry to the right logical qubits reads

$$\begin{aligned}\eta_{ZZX}^{\text{even}} X_{\text{right}}^1 \eta_{ZZX}^{\text{even}} &= \left(\prod_{j \in \text{even}} X_j \right) X_{2L} Z_{2L-1} \left(\prod_{j \in \text{even}} X_j \right) \\ &= X_{2L} X_{2L} Z_{2L-1} X_{2L} = X_{2L} Z_{2L-1} = X_{\text{left}}^1\end{aligned}\quad (248)$$

and

$$\begin{aligned}\eta_{ZZX}^{\text{even}} Z_{\text{right}}^1 \eta_{ZZX}^{\text{even}} &= \left(\prod_{j \in \text{even}} X_j \right) Z_{2L} \left(\prod_{j \in \text{even}} X_j \right) \\ &= X_{2L} Z_{2L} X_{2L} = -X_{2L} Z_{2L} X_{2L} = -Z_{\text{right}}^1.\end{aligned}\quad (249)$$

Then, the representation of the $\mathbb{Z}_{ZZ}^{\text{even}}$ symmetry at the right edge is given by

$$U_{\text{right}}(\eta_{ZZX}^{\text{even}}) = X_{\text{right}}. \quad (250)$$

The action of the $\mathbb{Z}_{ZZ}^{\text{odd}}$ symmetry to the right logical qubits reads

$$\begin{aligned}\eta_{ZZX}^{\text{odd}} X_{\text{right}}^1 \eta_{ZZX}^{\text{odd}} &= \left(\prod_{j \in \text{odd}} X_j \right) X_{2L} Z_{2L-1} \left(\prod_{j \in \text{odd}} X_j \right) \\ &= X_{2L-1} X_{2L} Z_{2L-1} X_{2L-1} = X_{2L} Z_{2L-1} \\ &= -X_{\text{right}}^1\end{aligned}\quad (251)$$

and

$$\begin{aligned}\eta_{ZZX}^{\text{odd}} Z_{\text{right}}^1 \eta_{ZZX}^{\text{odd}} &= \left(\prod_{j \in \text{odd}} X_j \right) Z_{2L} \left(\prod_{j \in \text{odd}} X_j \right) \\ &= X_{2L-1} Z_{2L} X_{2L-1} = Z_{2L} = Z_{\text{right}}^1.\end{aligned}\quad (252)$$

Then, the representation of the $\mathbb{Z}_{ZZ}^{\text{odd}}$ symmetry at the right edge is given by

$$U_{\text{right}}(\eta_{ZZX}^{\text{odd}}) = Z_{\text{right}}. \quad (253)$$

C. Ising gate

The controlled phase shift gate is decomposed by using the Z gate and the Ising gate as

$$\text{CP}(\phi_j) = e^{-i\frac{\phi_j}{4}} e^{i\frac{\phi_j}{4} Z_j \otimes I_{j+1}} e^{i\frac{\phi_j}{4} I_j \otimes Z_{j+1}} e^{-i\frac{\phi_j}{4} Z_j \otimes Z_{j+1}}. \quad (254)$$

In actual experiments, the CZ gate and the CP gate are constructed by using this formula. The product of the CP gate is

$$\prod_{j=1}^{2L} \text{CP}(\phi_j) = \prod_{j=1}^{2L} e^{-i\frac{\phi_j}{4}} e^{i\frac{(\phi_{j-1} + \phi_j)}{4} Z_j} e^{-i\frac{\phi_j}{4} Z_j \otimes Z_{j+1}} \quad (255)$$

for a closed chain, and

$$\begin{aligned}&\prod_{j=1}^{2L-1} \text{CP}(\phi_j) \\ &= e^{i\frac{\phi_1}{4} Z_1} e^{i\frac{\phi_{2L}}{4} Z_{2L}} \prod_{j=2}^{2L-1} e^{-i\frac{\phi_j}{4}} e^{i\frac{(\phi_{j-1} + \phi_j)}{4} Z_j} e^{-i\frac{\phi_j}{4} Z_j \otimes Z_{j+1}}\end{aligned}\quad (256)$$

for an open chain.

In general, it is hard to tune the angles of the Z gate and the Ising gate. By generalizing (256), it is natural to consider independent angles for the Z gate and the ZZ Ising gate as

$$\text{ZZ} \equiv \prod_{j=1}^{2L} e^{i\frac{\phi_j^Z}{4} Z_j} \prod_{j=1}^{2L-1} e^{-i\frac{\phi_j^{ZZ}}{4} Z_j \otimes Z_{j+1}}. \quad (257)$$

The cluster state is generated by

$$|\mathcal{C}(\{\phi_j^Z, \phi_j^{ZZ}\})\rangle \equiv \text{ZZ} \bigotimes_{j=1}^L |+\rangle. \quad (258)$$

The corresponding Hamiltonian is given by

$$\mathcal{H}_{\text{CP}} = \alpha_{\zeta_{j-1} \zeta_{j+1}} Z_{j-1}^{\zeta_{j-1}} X_j Z_{j+1}^{\zeta_{j+1}} + \beta_{v_{j-1} v_{j+1}} Y_{j-1}^{v_{j-1}} X_j Y_{j+1}^{v_{j+1}} \quad (259)$$

with

$$\alpha_{00} = 0, \quad (260)$$

$$\alpha_{10} = \alpha_{01} = \frac{\sin^2 \frac{\phi_j^Z}{2}}, \quad (261)$$

$$\alpha_{11} = -\sin^2 \frac{\phi_j^Z}{2} \cos \phi, \quad (262)$$

$$\beta_{00} = \cos^2 \frac{\phi}{2} \sin \phi, \quad (263)$$

$$\beta_{10} = \beta_{01} = -\frac{\sin 2\phi}{4}, \quad (264)$$

$$\beta_{11} = -\sin^2 \frac{\phi}{2} \sin \phi. \quad (265)$$

1. Cross-resonance gate

The cross-resonance gate is defined by[53]

$$\begin{aligned}U_{\text{CR}} &\equiv e^{-i\frac{\phi_j^{\text{CR}}}{2} Z_j \otimes X_{j+1}} \\ &= \frac{1}{\sqrt{2}} \begin{pmatrix} \cos \frac{\phi_j^{\text{CR}}}{2} & -i \sin \frac{\phi_j^{\text{CR}}}{2} & 0 & 0 \\ -i \sin \frac{\phi_j^{\text{CR}}}{2} & \cos \frac{\phi_j^{\text{CR}}}{2} & 0 & 0 \\ 0 & 0 & \cos \frac{\phi_j^{\text{CR}}}{2} & i \sin \frac{\phi_j^{\text{CR}}}{2} \\ 0 & 0 & i \sin \frac{\phi_j^{\text{CR}}}{2} & \cos \frac{\phi_j^{\text{CR}}}{2} \end{pmatrix},\end{aligned}\quad (266)$$

which is naturally equipped in transmon-type superconducting qubits. By applying the Hadamard gate to the $(j+1)$ -th bit, we obtain the Ising gate.

2. Mølmer-Sørensen gate

The Mølmer-Sørensen gate is defined by[56]

$$\begin{aligned}
 U_{\text{MS}} &\equiv e^{-i\frac{\phi_j^{\text{MS}}}{2}X_j \otimes X_{j+1}} \\
 &= \frac{1}{\sqrt{2}} \begin{pmatrix} \cos \frac{\phi_j^{\text{MS}}}{2} & 0 & 0 & -i \sin \frac{\phi_j^{\text{MS}}}{2} \\ 0 & \cos \frac{\phi_j^{\text{MS}}}{2} & -i \sin \frac{\phi_j^{\text{MS}}}{2} & 0 \\ 0 & i \sin \frac{\phi_j^{\text{MS}}}{2} & \cos \frac{\phi_j^{\text{MS}}}{2} & 0 \\ i \sin \frac{\phi_j^{\text{MS}}}{2} & 0 & 0 & \cos \frac{\phi_j^{\text{MS}}}{2} \end{pmatrix}, \tag{267}
 \end{aligned}$$

which is naturally equipped in qubits made of ion trap. By applying the Hadamard gate to the j -th and $(j + 1)$ -th bits, we obtain the Ising gate.

-
- [1] R. Feynman, Simulating physics with computers, *Int. J. Theor. Phys.* **21**, 467 (1982).
- [2] D. P. DiVincenzo, Quantum Computation, *Science* **270**, 255 (1995).
- [3] M. Nielsen and I. Chuang, *Quantum Computation and Quantum Information*, Cambridge University Press, (2016); ISBN 978-1-107-00217-3.
- [4] D. Deutsch, Quantum Theory, the Church-Turing Principle and the Universal Quantum Computer, *Proceedings of the Royal Society A*. **400**, 97 (1985).
- [5] C. M. Dawson and M. A. Nielsen, The Solovay-Kitaev algorithm, *Quantum Information and Computation* **6**, 81 (2006).
- [6] M. Nielsen and I. Chuang, *Quantum Computation and Quantum Information*, Cambridge University Press, Cambridge, UK (2010).
- [7] Robert Raussendorf and Hans J. Briegel, A One-Way Quantum Computer, *Phys. Rev. Lett.* **86**, 5188 (2019)
- [8] R. Raussendorf, D. E. Browne, and H. J. Briegel, Measurement-based quantum computation on cluster states, *Physical Review A* **68**, 022312 (2003).
- [9] Hans J. Briegel and Robert Raussendorf, Persistent Entanglement in Arrays of Interacting Particles, *Phys. Rev. Lett.* **86**, 910 (2001)
- [10] W. Son, L. Amico, and V. Vedral, Topological order in 1D cluster state protected by symmetry, *Quantum Inf. Process.* **11**, 1961 (2012).
- [11] M. A. Nielsen, Cluster-state quantum computation, *Rep. Math. Phys.* **57**, 147 (2006).
- [12] Z.-C. Gu and X.-G. Wen, Tensor-entanglement-filtering renormalization approach and symmetry-protected topological order, *Phys. Rev. B* **80**, 155131 (2009).
- [13] F. Pollmann, A. M. Turner, E. Berg, and M. Oshikawa, Entanglement spectrum of a topological phase in one dimension, *Phys. Rev. B* **81**, 064439 (2010).
- [14] Xie Chen, Zheng-Cheng Gu, and Xiao-Gang Wen, Local unitary transformation, long-range quantum entanglement, wave function renormalization, and topological order
- [15] Dawid Paszko, Dominic C. Rose, Marzena H. Szymanska, and Arijeet Pal, Edge Modes and Symmetry-Protected Topological States in Open Quantum Systems, *Phys. Rev. X Quantum* **5**, 030304 (2024)
- [16] Dominic V. Else, Ilai Schwarz, Stephen D. Bartlett, and Andrew C. Doherty, Symmetry-Protected Phases for Measurement-Based Quantum Computation, *Phys. Rev. Lett.* **108**, 240505 (2012).
- [17] Sahand Seifnashri and Shu-Heng Shao, Cluster State as a Non-invertible Symmetry-Protected Topological Phase, *Phys. Rev. Lett.* **133**, 116601 (2024)
- [18] A. Parayil Mana, Y. Li, H. Sukeno, and T.-C. Wei, Kennedy-Tasaki transformation and non-invertible symmetry in lattice models beyond one dimension, *Phys. Rev. B* **109**, 245129 (2024).
- [19] Xie Chen, Zheng-Cheng Gu, and Xiao-Gang Wen, Classification of gapped symmetric phases in one-dimensional spin systems, *Phys. Rev. B* **83**, 035107 (2011)
- [20] Dominic V. Else and Chetan Nayak, Classifying symmetry-protected topological phases through the anomalous action of the symmetry on the edge, *Phys. Rev B* **90**, 235137 (2014)
- [21] Nathan Seiberg, Shu-Heng Shao, Majorana chain and Ising model (non-invertible) translations, anomalies, and emanant symmetries, *SciPost Phys.* **16**, 064 (2024)
- [22] Nathan Seiberg, Sahand Seifnashri and Shu-Heng Shao, Non-invertible symmetries and LSM-type constraints on a tensor product Hilbert space, *SciPost Phys.* **16**, 154 (2024)
- [23] I. Schwartz, D. Cogan, E. R. Schmidgall, Y. Don, L. Gantz, O. Kenneth, N. H. Lindner, D. Gershoni, Deterministic Generation of a Cluster State of Entangled Photons, *Science* **354**, 434 (2016)
- [24] Ruizhe Shen, Tianqi Chen, Bo Yang, Yin Zhong and Ching Hua Lee, Robust simulations of many-body symmetry-protected topological phase transitions on a quantum processor, *npj quantum information*, **11**, 179 (2025)
- [25] M. Hein, W. Dur, J. Eisert, R. Raussendorf, M. V. den Nest, and H.-J. Briegel, Entanglement in Graph States and its Applications (2006), arXiv:quant-ph/0602096.
- [26] Daniel Gottesman, Stabilizer Codes and Quantum Error Correction, arXiv:quant-ph/9705052
- [27] Ian Affleck, Tom Kennedy, Elliott H. Lieb, and Hal Tasaki, Rigorous results on valence-bond ground states in antiferromagnets, *Phys. Rev. Lett.* **59**, 799 (1987)
- [28] Ian Affleck, Tom Kennedy, Elliott H. Lieb, and Hal Tasaki, Valence bond ground states in isotropic quantum antiferromagnets

- nets, *Commun. Math. Phys.* 115, 477 (1988)
- [29] A. Kitaev, Fault-tolerant quantum computation by anyons, *Annals of Physics* 303, 2 (2003)
- [30] T. Kennedy and H. Tasaki, Hidden symmetry breaking and the haldane phase in $s = 1$ quantum spin chains, *Commun. Math. Phys.* 147, 431 (1992)
- [31] T. Kennedy and H. Tasaki, Hidden $Z_2 \times Z_2$ symmetry breaking in haldane-gap antiferromagnets, *Phys. Rev. B* 45, 304 (1992)
- [32] M. Oshikawa, Hidden $Z_2 \times Z_2$ symmetry in quantum spin chains with arbitrary integer spin, *J. Phys.: Condens. Matter* 4, 7469 (1992).
- [33] L. Li, M. Oshikawa, and Y. Zheng, Noninvertible duality transformation between symmetry-protected topological and spontaneous symmetry breaking phases, *Phys. Rev. B* 108, 214429 (2023).
- [34] G. Hooft, Naturalness, chiral symmetry, and spontaneous chiral symmetry breaking, in *Recent Developments in Gauge Theories* (Springer, Berlin, 1980) pp. 135–157.
- [35] Michael J. Bremner, Richard Jozsa, Dan J. Shepherd, Classical simulation of commuting quantum computations implies collapse of the polynomial hierarchy, *Proc. A* 467, 459 (2011)
- [36] Ruben Verresen, Roderich Moessner, and Frank Pollmann, One-dimensional symmetry protected topological phases and their transitions, *Phys. Rev. B* 96, 165124 (2017).
- [37] Sadaf F, V. Subrahmanyam, Quantum correlations in a cluster spin model with three-spin interactions, arXiv:2503.14060
- [38] Zhian Jia, Generalized cluster states from Hopf algebras: non-invertible symmetry and Hopf tensor network representation, *J. High Energy Phys.* 2024, 147 (2024)
- [39] Zhian Jia, Weak Hopf non-invertible symmetry-protected topological spin liquid and lattice realization of (1+1)D symmetry topological field theory, arXiv:2412.15336
- [40] W. Dur, L. Hartmann, M. Hein, M. Lewenstein, and H.-J. Briegel, Entanglement in Spin Chains and Lattices with Long-Range Ising-Type Interactions, *Phys. Rev. Lett.* 94, 097203 (2005).
- [41] L. Hartmann, J. Calsamiglia, W. Dur and H. J. Briegel, Weighted graph states and applications to spin chains, lattices and gases, *J. Phys. B: At. Mol. Opt. Phys.* 40 S1 (2007)
- [42] Tomohiro Yamazaki and Yuki Takeuchi, Measurement-based quantum computation on weighted graph states with arbitrarily small weight, arXiv:2512.01327
- [43] Jieshan Huang Yulin Chi, Yan Li, Xudong Li, Xiaojiong Chen, Chonghao Zhai, Yun Zheng, Qiongyi He, Qihuang Gong and Jianwei Wang, Demonstration of hypergraph-state quantum information processing, *Nat. Com.* 15, 2601 (2024)
- [44] M. Rossi, M. Huber, D. Bruss and C. Macchiavello, Quantum hypergraph states, *New J. Phys.* 15 113022 (2013)
- [45] Weiguang Cao, Masahito Yamazaki, and Linhao Li, Duality viewpoint of noninvertible symmetry protected topological phases, arXiv:2502.20435
- [46] Linhao Li, Rui-Zhen Huang, and Weiguang Cao, Noninvertible symmetry-enriched quantum critical point, *Phys. Rev. B* 112, L081113 (2025)
- [47] Kazuhiko Minami, Infinite number of solvable generalizations of XY-chain, with cluster state, and with central charge $c = m/2$ *Nuclear Physics B* 925, 144 (2017)
- [48] Yuji Yanagihara and Kazuhiko Minami, Exact solution of a cluster model with next-nearest-neighbor interaction, *Prog. Theor. Exp. Phys.* 113A01 (2020)
- [49] Christopher Fechisin, Nathanan Tantivasadakarn, and Victor V. Albert, Noninvertible Symmetry-Protected Topological Order in a Group-Based Cluster State, *Phys. Rev. X* 15, 011058 (2025)
- [50] D. Gross and J. Eisert, Novel Schemes for Measurement-Based Quantum Computation, *Phys. Rev. Lett.* 98, 220503 (2007)
- [51] Sergei Bravyi, Alexei Kitaev, Universal quantum computation with magic states, *Phys. Rev. A* 71, 022316 (2005)
- [52] D. Gross and J. Eisert, Measurement-based quantum computation beyond the one-way model, *Phys. Rev. A* 76, 052315 (2007)
- [53] A. D. Corcoles, E. Magesan, S. J. Srinivasan, A. W. Cross, M. Steffen, J. M. Gambetta and J. M. Chow, Demonstration of a quantum error detection code using a square lattice of four superconducting qubits, *Nat. Com.* 6, 6979 (2015).
- [54] Jerry M. Chow, A. D. Corcoles, Jay M. Gambetta, Chad Rigetti, B. R. Johnson, John A. Smolin, J. R. Rozen, George A. Keefe, Mary B. Rothwell, Mark B. Ketchen, M. Steffen, A simple all-microwave entangling gate for fixed-frequency superconducting qubits, *Phys. Rev. Lett.* 107, 080502 (2011)
- [55] A. D. Corcoles, Jay M. Gambetta, Jerry M. Chow, John A. Smolin, Matthew Ware, J. D. Strand, B. L. T. Plourde, M. Steffen, Process verification of two-qubit quantum gates by randomized benchmarking, *Phys. Rev. A* 87, 030301(R) (2013)
- [56] A. Sorensen and K. Molmer, Quantum computation with Ions in thermal motion, *Phys. Rev. Lett.* 82, 1971 (1999); Multiparticle Entanglement of Hot Trapped Ions, Klaus Molmer and Anders Sorensen, *Phys. Rev. Lett.* 82, 1835 (1999).
- [57] Ferdinand Schmidt-Kaler, Hartmut Haffner, Mark Riebe, Stephan Gulde, Gavin P. T. Lancaster, Thomas Deuschle, Christoph Becher, Christian F. Roos, Jurgen Eschner and Rainer Blatt Realization of the Cirac-Zoller controlled-NOT quantum gate *Nature* 422, 408 (2003)
- [58] Yuan Xu, Yuwei Ma, Weizhou Cai, Xianghao Mu, Wei Dai, Weiting Wang, Ling Hu, Xuegang Li, Jiaxiu Han, Haiyan Wang, Yipu Song, Zhen-Biao Yang, Shi-Biao Zheng, Luyan Sun, Demonstration of Controlled-Phase Gates between Two Error-Correctable Photonic Qubits, *Phys. Rev. Lett.* 124, 120501 (2020)
- [59] Stefan Krastanov, Kurt Jacobs, Gerald Gilbert, Dirk R. Englund and Mikkel Heuck, Controlled-phase gate by dynamic coupling of photons to a two-level emitter *npj Quantum Information* 8, 103 (2022)
- [60] Chenhui Wang, Weilong Wang, Yangyang Fei, Zhiqiang Fan, Hanshi Zhao, Yuyan Mage, Zheng Shan, Time-frequency Entangled Photon Mediated CCZ Gate, arXiv:2509.06497
- [61] Hao-Tian Liu, Bing-Jie Chen, Jia-Chi Zhang, Yong-Xi Xiao, Tian-Ming Li, Kaixuan Huang, Ziting Wang, Hao Li, Kui Zhao, Yueshan Xu, Cheng-Lin Deng, Gui-Han Liang, Zheng-He Liu, Si-Yun Zhou, Cai-Ping Fang, Xiaohui Song, Zhongcheng Xiang, Dongning Zheng, Yun-Hao Shi, Kai Xu, Heng Fan, Direct Implementation of High-Fidelity Three-Qubit Gates for Superconducting Processor with Tunable Couplers, *Phys. Rev. Lett.* 135, 050602 (2025)
- [62] Katrin Bolsmann, Thiago L. M. Guedes, Weibin Li, Joseph, W. P. Wilkinson, Igor Lesanovsky, and Markus Muller, Fast Native Three-Qubit Gates and Fault-Tolerant Quantum Error Correction with Trapped Rydberg Ions, arXiv:2512.16641
- [63] Niklas J. Glaser, Federico Roy, and Stefan Filipp, Controlled-Controlled-Phase Gates for Superconducting Qubits Mediated by a Shared Tunable Coupler, *Phys. Rev. Appl.* 19, 044001 (2023)
- [64] Gerard Pelegri Andrew J. Daley, Jonathan D. Pritchard, High-fidelity multiqubit Rydberg gates via two-photon adiabatic rapid passage, *Quantum Sci. Technol.* 7, 045020 (2022)
- [65] Ming Xue, Shijie Xu, Xinwei Li, Xiangliang Li, High-fidelity and robust controlled-Z gates implemented with Rydberg atoms via echoing rapid adiabatic passage, *Phys. Rev. A* 110, 032619

(2024)